Université ABBES LAGHROUR Khenchela
جامعة عباس لغرور خنشلة

Faculté des Sciences et de la Technologie
كلية العلوم والتكنولوجيا

Département de Génie Electrique
قسم الهندسة الكهربائية

N° Série : .....

Mémoire de fin d'étude

Pour l'obtention du diplôme de Master

Filière : Automatique

Spécialité : Automatique et Informatique Industrielle

Adaptive Blood Glucose Control Control: for Type 1 Diabetes

Présenté par

BADAOUI Oussama

Soutenu le : 14/06/2026 devant les Membres du jury :

Mme. BESSAM Besma	MCA	Université Abbes Laghrour Khenchela	Présidente
Mr. MOKHTARI Khalil	MCB	Université Abbes Laghrour Khenchela	Encadrant
Mme. AOURAR Salima	MAA	Université Abbes Laghrour Khenchela	Examinatrice

Promotion 2025/2026

Dédicace

Je dédie ce mémoire :

À ma chère mère, pour son amour inconditionnel, ses sacrifices, ses prières et son soutien indéfectible tout au long de mon parcours.

À la mémoire de mon père, dont les valeurs, les conseils et l'exemple continuent de guider mes pas et d'inspirer ma persévérance.

À mon épouse, pour sa patience, sa compréhension et son soutien constant durant les périodes de travail et de recherche.

À mon enfant, source de bonheur, d'espoir et de motivation pour construire un avenir meilleur.

À mes frères et à toute ma famille, pour leurs encouragements et leur confiance.

À tous ceux qui ont contribué, de près ou de loin, à ma formation et à mon épanouissement personnel et professionnel.

Je leur exprime toute ma gratitude et leur dédie humblement ce mémoire. ...

Remerciement

Avant tout, je remercie Allah, le Tout-Puissant, de m'avoir accordé la santé, la volonté et la persévérance nécessaires pour mener à bien ce travail.

Je tiens à exprimer ma profonde gratitude à mon encadreur pour sa disponibilité, ses précieux conseils, son accompagnement scientifique et les orientations pertinentes qu'il m'a apportées tout au long de la réalisation de ce mémoire. Mes sincères remerciements s'adressent également aux membres du jury qui ont accepté d'évaluer ce travail et de consacrer une partie de leur temps à son examen.

J'adresse également mes remerciements à l'ensemble des enseignants du département de Génie Électrique pour la qualité de la formation qu'ils m'ont dispensée et pour les connaissances qu'ils m'ont transmises au cours de mon parcours universitaire.

Je remercie particulièrement ma mère pour son soutien inconditionnel, ses encouragements permanents et ses prières qui ont toujours été une source de force et de motivation. J'adresse une pensée respectueuse à la mémoire de mon père, dont les valeurs et les enseignements continuent de m'accompagner dans chaque étape de ma vie.

Mes remerciements vont également à mon épouse et à mon enfant pour leur patience, leur compréhension et leur soutien moral tout au long de cette période d'études et de recherche. Enfin, je remercie ma famille, mes amis, mes collègues ainsi que toutes les personnes qui ont contribué, directement ou indirectement, à l'aboutissement de ce travail.

À toutes et à tous, j'exprime ma sincère reconnaissance.

Résumé

Le diabète de type 1 (DT1) résulte de la destruction auto-immune des cellules β du pancréas, supprimant la sécrétion endogène d'insuline et imposant une insulinothérapie exogène permanente. Le système de pancréas artificiel (SPA) automatise ce traitement grâce à un algorithme en boucle fermée qui régule l'administration d'insuline à partir de mesures continues de la glycémie. La conception d'un contrôleur fiable pour le SPA est rendue difficile par la non-linéarité inhérente du système glucose–insuline, la variabilité physiologique significative inter- et intra-patients, ainsi que les perturbations continues liées aux repas et à l'activité physique. Les approches existantes manquent soit de garanties formelles de stabilité, soit nécessitent une connaissance explicite des paramètres du patient, soit imposent une charge de calcul prohibitive pour une mise en œuvre embarquée.

Ce travail propose l'application du **Contrôle Adaptatif Simple** (CAS) à la régulation de la glycémie dans le DT1. Le CAS est une stratégie de contrôle adaptatif à modèle de référence direct qui adapte une matrice de gains en temps réel à partir de la seule erreur de suivi de sortie mesurable, sans identificateur de paramètres, sans observateur d'état et sans connaissance des paramètres physiologiques du patient. La plante est décrite par le modèle minimal de Bergman étendu à quatre états, exprimé sous la forme $\dot{x}_p = A_p(x_p)x_p + B_p u$. La stabilité en boucle fermée est établie dans le cadre de la Passivité Presque Stricte (PPS) : un Compensateur par Avance Parallèle dynamique rend le système augmenté PPS, et un théorème de Lyapunov démontre le bornage uniforme de tous les signaux et la convergence asymptotique de l'erreur de suivi. Le contrôleur est validé par trois études de simulation couvrant dix patients virtuels avec $\pm 30\%$ d'incertitude paramétrique, dix scénarios cliniques de la normoglycémie à l'hyperglycémie critique, et un protocole sur une journée complète avec trois repas. La glycémie est maintenue dans la zone sûre $[70, 180]$ mg/dL dans tous les cas sans épisode hypoglycémique, confirmant la fiabilité clinique et l'efficacité computationnelle de l'approche proposée.

Mots clés: Diabète de type 1, Pancréas artificiel, Régulation de la glycémie, Contrôle adaptatif simple, Modèle minimal de Bergman, Passivité presque stricte, Stabilité de Lyapunov, Variabilité inter-patients.

Abstract

Type 1 Diabetes Mellitus (T1DM) results from the autoimmune destruction of pancreatic β-cells, eliminating endogenous insulin secretion and requiring permanent exogenous insulin administration. The Artificial Pancreas System (APS) automates this therapy through a closed-loop algorithm that continuously regulates insulin delivery from glucose sensor measurements. Designing a reliable APS controller is challenging due to the inherent nonlinearity of the glucose–insulin system, significant inter- and intra-patient physiological variability, and continuous meal and activity disturbances. Existing approaches either lack formal stability guarantees, require explicit knowledge of patient parameters, or are computationally prohibitive for embedded implementation.

This thesis proposes the application of **Simple Adaptive Control** (SAC) to blood glucose regulation in T1DM. SAC is a direct Model Reference Adaptive Control strategy that adapts a gain matrix in real time from the measurable output tracking error alone, requiring no plant identifier, no state observer, and no knowledge of the patient's physiological parameters. The plant is described by the extended four-state Bergman Minimal Model, cast in the nonlinear state-space form $\dot{x}_p = A_p(x_p)x_p + B_p u$. Closed-loop stability is established via the Almost Strict Passivity (ASP) framework: a dynamic Parallel Feedforward Compensator renders the augmented plant ASP, and a Lyapunov-based theorem proves uniform boundedness of all closed-loop signals and asymptotic convergence of the tracking error. The controller is validated through three simulation studies covering ten virtual patients with $\pm 30\%$ parameter uncertainty, ten clinical scenarios from normal fasting to critical hyperglycaemia, and a full-day three-meal protocol. Blood glucose is maintained within the safe zone $[70, 180]$ mg/dL in all cases with no hypoglycaemic events, confirming the clinical reliability and computational efficiency of the proposed approach.

Keywords: Type 1 Diabetes Mellitus, Artificial Pancreas, Blood Glucose Regulation, Simple Adaptive Control, Bergman Minimal Model, Almost Strict Passivity, Parallel Feedforward Compensator, Lyapunov Stability, Inter-Patient Variability.

Contents

List of Figures

List of Tables

List of Symbols

Symbol	Description	Unit
State Variables		
$G(t)$	Blood glucose (plasma) concentration	mg/dL
$X(t)$	Remote (interstitial) insulin effect	min^{-1}
$I(t)$	Plasma insulin concentration	mU/L
$D(t)$	Meal glucose disturbance rate	mg/dL/min
$x_p(t)$	Plant state vector, $[G,\, X,\, I,\, D]^\mathsf{T}$	–
$x_m(t)$	Reference model state vector	–
Physiological Constants and Parameters		
G_b	Basal (target) plasma glucose concentration	mg/dL
I_b	Basal plasma insulin concentration	mU/L
p_1	Glucose effectiveness (insulin-independent uptake)	min^{-1}
p_2	Remote-insulin decay rate	min^{-1}
p_3	Insulin-dependent glucose uptake gain	$\mu\text{U}\,\text{mL}^{-1}\,\text{min}^{-2}$
p_4	Plasma insulin clearance rate	min^{-1}
p_5	Meal disturbance decay rate	min^{-1}
t	Time	min
Control Inputs and Outputs		
$u(t)$	Exogenous insulin infusion rate (control input)	mU/min
$u_m(t)$	Reference model input command	mg/dL
$u_{\max}$	Maximum admissible insulin infusion rate	mU/min

(continued on next page)

(continued from previous page)

Symbol	Description	Unit
$y(t)$	Plant output (measured glucose)	mg/dL
$y_m(t)$	Reference model output	mg/dL
$y_a(t)$	Augmented plant output, $y_a = y_p + v$	mg/dL
$y_p(t)$	Plant (Bergman model) output	mg/dL
$v(t)$	PFC output signal	mg/dL
Error Signals		
$e_y(t)$	Output tracking error, $e_y = y_m - y_a$	mg/dL
$e_x(t)$	State error vector, $e_x = x_m - x_p$	–
$\widetilde{K}_I(t)$	Adaptive gain error, $\widetilde{K}_I = K_I - K_e$	–
$d_i(x_p, t)$	Bounded input disturbance	–
$d_o(x_p, t)$	Bounded output disturbance	–
$F(t)$	Bounded disturbance bias term in $\dot{V}$	–
SAC Controller		
$K(t)$	Adaptive gain matrix, $K = K_I + K_P$	–
$K_I(t)$	Integral component of adaptive gain	–
$K_P(t)$	Proportional component of adaptive gain	–
K_e	Unknown stabilising (ASP) gain matrix	–
K_{I0}	Initial value of integral gain	–
$r(t)$	SAC regressor vector, $r^\mathsf{T} = [e_y,\, x_m^\mathsf{T},\, u_m]$	–
Γ	Integral gain adaptation weight ($\Gamma = 20$)	–
$\bar{\Gamma}$	Proportional gain adaptation weight ($\bar{\Gamma} = 5$)	–
σ	Leakage coefficient ($\sigma = 0.05$)	–
State-Space Matrices		
$A_p(x_p)$	State-dependent system matrix of the plant	–

(continued on next page)

(continued from previous page)

Symbol	Description	Unit
B_p	Input matrix of the plant	–
C_p	Output matrix of the plant	–
A_m	State matrix of the reference model	–
B_m	Input matrix of the reference model	–
C_m	Output matrix of the reference model	–
$A_{pc}(x_p)$	Closed-loop state matrix under feedback K_e	–
$P(x_p)$	Lyapunov matrix (positive definite)	–
$Q(x_p)$	Negative-definite matrix in Lyapunov equation	–
Transfer Functions and Operators		
$G_p(s)$	Transfer function of the Bergman plant	–
$G_a(s)$	Transfer function of the augmented plant	–
$H(s)$	Stabilising controller transfer function	–
$H^{-1}(s)$	Parallel feedforward compensator (PFC)	–
$W_m(s)$	Reference model transfer function, $1/(s+1)$	–
s	Complex Laplace variable	min^{-1}
τ_m	Reference model time constant ($\tau_m = 1\,\mathrm{min}$)	min
Stability and Performance		
$V(e_x, \widetilde{K}_I)$	Composite Lyapunov function candidate	–
$\dot{V}(t)$	Time derivative of the Lyapunov function	–
$\alpha_1, \ldots, \alpha_6$	Positive bounding constants in $\dot{V}$ inequality	–
n_p	Order (dimension) of the plant	–
n_m	Order (dimension) of the reference model	–
n	State dimension of the plant	–
m	Input/output dimension	–

(continued on next page)

(continued from previous page)

Symbol	Description	Unit
Physiological Modeling (Chapter 2)		
$R_a(t)$	Rate of glucose appearance from meal absorption	mg/dL/min
$EGP(t)$	Endogenous glucose production rate	mg/dL/min
$U_g(t)$	Rate of glucose utilization by tissues	mg/dL/min
$E(t)$	Renal glucose excretion rate	mg/dL/min
$x_i(t)$	i-th state variable of the Bergman model, $i = 1, \ldots, 4$	–
$\dot{x}_i(t)$	Time derivative of x_i	(unit of x_i)/min
Performance Indices		
ISE	Integral of Squared Error, $\int e_y^2 \, dt$	$\text{mg}^2/\text{dL}^2 \cdot \text{min}$
IAE	Integral of Absolute Error, $\int \lvert e_y \rvert \, dt$	mg/dL·min
ITAE	Integral of Time-weighted Absolute Error, $\int t \lvert e_y \rvert \, dt$	$\text{mg/dL} \cdot \text{min}^2$

List of Abbreviations

Abbreviation	Definition
Medical and Clinical	
ADA	American Diabetes Association
APS	Artificial Pancreas System
BGL	Blood Glucose Level
CGM	Continuous Glucose Monitor
DT1	Diabète de Type 1 (French equivalent of T1DM)
FDA	U.S. Food and Drug Administration
IVGTT	Intravenous Glucose Tolerance Test
T1DM	Type 1 Diabetes Mellitus
T2DM	Type 2 Diabetes Mellitus
TIR	Time In Range (percentage of time in $[70, 180]$ mg/dL)
WHO	World Health Organization
Control Theory	
AP	Artificial Pancreas
ASP	Almost Strictly Passive (system property)
DBST	Dynamical Backstepping Controller
FBL	Feedback Linearisation
HOSMC	Higher-Order Sliding Mode Control
IAE	Integral of Absolute Error
ISE	Integral of Squared Error
ITAE	Integral of Time-weighted Absolute Error

(continued on next page)

(continued from previous page)

Abbreviation	Definition
LPV	Linear Parameter Varying
LTI	Linear Time-Invariant
MIMO	Multi-Input Multi-Output
MPC	Model Predictive Control
MRAC	Model Reference Adaptive Control
ODE	Ordinary Differential Equation
PFC	Parallel Feedforward Compensator
PID	Proportional-Integral-Derivative
SAC	Simple Adaptive Control
SISO	Single-Input Single-Output
SMC	Sliding Mode Control
SP	Strictly Passive
Modeling	
BMM	Bergman Minimal Model
CVGA	Control Variability Grid Analysis
EGP	Endogenous Glucose Production
ISI	Insulin Sensitivity Index

Chapter 1

General Introduction and Background

1.1 Context and Motivation

Diabetes mellitus is one of the leading chronic metabolic diseases of the modern era and has become a major global public health burden. According to the International Diabetes Federation, the prevalence of diabetes in the world population reached 9.3%, corresponding to approximately 463 million people, in 2019, and is projected to rise to 10.2% (578 million) by 2030 and 10.9% (700 million) by 2045 [11]. Diabetes is consistently ranked among the top ten causes of death in adults worldwide and imposes immense socioeconomic costs through its associated complications and long-term disability [1].

Among the several forms of diabetes, *Type 1 Diabetes Mellitus* (T1DM) is an autoimmune disease characterised by the progressive destruction of the insulin-producing β-cells of the pancreatic islets of Langerhans by the patient's own immune system [12]. The result is a near-total loss of endogenous insulin secretion and a lifelong dependence on exogenous insulin therapy. Unlike Type 2 diabetes, which is primarily associated with insulin resistance and is strongly linked to lifestyle factors, T1DM arises predominantly in childhood and adolescence and has a genetic as well as environmental aetiology that is not yet fully understood.

In a healthy individual, the pancreas continuously monitors blood glucose concentration (BGC) and secretes insulin into the portal circulation in a precisely regulated manner. Insulin enables glucose uptake by peripheral tissues (muscle, adipose, liver), thereby lowering blood glucose to its fasting basal level of approximately 70–100 mg/dL. When blood glucose falls below this range, the α-cells of the pancreas secrete glucagon, stimulating hepatic glucose production and preventing hypoglycaemia. This bidirectional hormonal feedback loop maintains blood glucose within a remarkably narrow physiological window throughout the day [13].

In T1DM patients, the loss of β-cell function eliminates the insulin secretion arm of this

regulation loop entirely. Without exogenous insulin, blood glucose rises to dangerously high levels (hyperglycaemia, BGC $>$ 180 mg/dL), leading to acute complications such as diabetic ketoacidosis and, over the long term, to severe organ damage including retinopathy, nephropathy, peripheral neuropathy, and cardiovascular disease [10, 1]. Conversely, if too much insulin is administered, blood glucose drops below the safe threshold (hypoglycaemia, BGC $<$ 70 mg/dL), which can result in impaired cognitive function, seizures, loss of consciousness, and, in severe cases, death [14, 9].

The fundamental clinical challenge in T1DM management is therefore to maintain blood glucose continuously within the safe range $[70, 180]$ mg/dL, despite the continuous and unpredictable nature of disturbances (meals, physical activity, stress, illness) and the considerable variability in patients' physiological responses. Manual management through multiple daily injections and finger-stick glucose measurements is burdensome, imprecise, and frequently insufficient to prevent both hyperglycaemic and hypoglycaemic episodes [15].

These considerations have motivated decades of research into the *Artificial Pancreas System* (APS), an automated closed-loop device that continuously measures blood glucose using a sensor and automatically delivers the appropriate insulin dose through an infusion pump, guided by a control algorithm. The APS represents the most promising path toward the complete automation of insulin therapy for T1DM patients and has been the subject of intense investigation in both academic and industrial research since the early 1970s [16, 17, 18].

1.2 The Artificial Pancreas System

The artificial pancreas system, as illustrated in figure 1.1, consists of three principal hardware components working in a closed-loop configuration:

1. A **continuous glucose monitor (CGM)**, which measures the glucose concentration in the interstitial fluid at regular intervals (typically every 1–5 min) and transmits the readings wirelessly to the control unit.

2. A **control algorithm**, which processes the glucose measurements, compares them to the target setpoint ($G_b = 80$ mg/dL), and computes the appropriate insulin infusion command.

3. An **insulin pump**, which delivers subcutaneous insulin at the rate commanded by the algorithm.

The principle underlying the APS is directly analogous to the engineering concept of output feedback control: the controlled variable (blood glucose) is measured, the measurement is compared to a reference (the basal setpoint), and a control action (insulin infusion) is applied to drive the error to zero. However, the biological system being controlled is highly nonlinear, time-varying, subject to large and partially unpredictable disturbances, and characterised by significant inter- and intra-patient parameter variability. These characteristics make the APS control problem substantially more challenging than most classical industrial control problems and have motivated the development of advanced nonlinear and adaptive control strategies [1, 16].

Despite remarkable progress over the past two decades, including the FDA approval of several commercial hybrid closed-loop systems, the development of a fully automated and robust APS that operates safely across all daily life scenarios remains an open engineering challenge [17, 13].

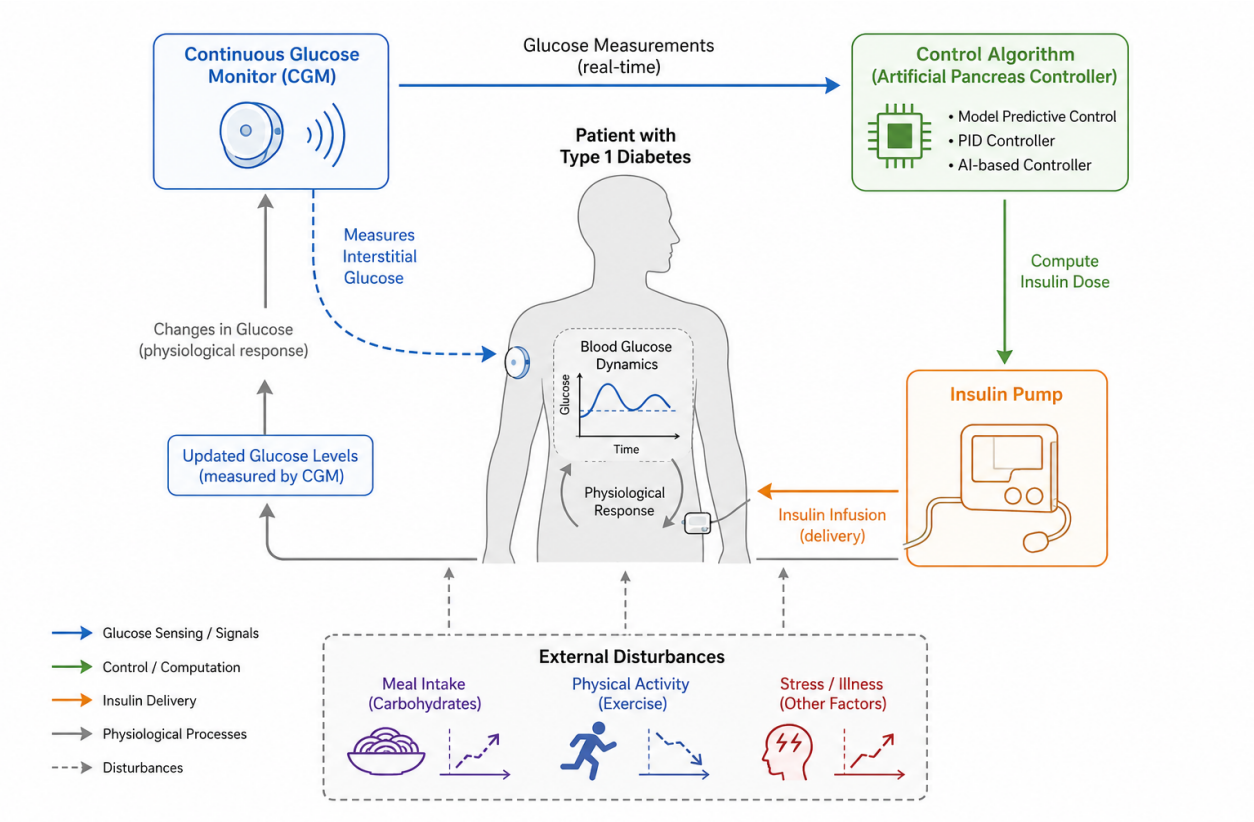

Figure 1.1: Closed-loop artificial pancreas system diagram

1.3 Mathematical Modeling of the Glucose–Insulin System

A reliable mathematical model of the glucose–insulin system is the cornerstone of any model-based APS control strategy. It enables the prediction of future glucose responses, the design of control laws, and the in silico evaluation of controller performance without exposing patients to risk.

1.3.1 Overview of Model Categories

Three decades of research have produced a rich body of mathematical models ranging from highly detailed physiological descriptions to parsimonious control-oriented representations. They can be broadly classified into the following categories [1, 2]:

Minimal models. The **Bergman Minimal Model** [6], derived from Intravenous Glucose Tolerance Test (IVGTT) experiments, describes glucose–insulin dynamics through three coupled differential equations representing plasma glucose, remote insulin action, and plasma insulin. It is the most widely used control-oriented model due to its physiological interpretability and mathematical simplicity. Extensions incorporating meal absorption dynamics [19] and an explicit plasma insulin compartment [9] constitute the four-state model adopted in this thesis.

Compartmental physiological models. The **Sorensen model** [3], the **Dalla Man model** [20], and the **Hovorka model** [4] incorporate multiple physiological compartments representing individual organs and metabolic pathways. They offer higher physiological fidelity, particularly for postprandial and subcutaneous-delivery scenarios, but their complexity limits their analytical tractability for controller design.

Population-based simulators. The **UVa/Padova Type 1 Diabetes Simulator** [5], accepted by the U.S. Food and Drug Administration (FDA) as a substitute for preclinical animal studies, represents a cohort of 30 virtual subjects and enables statistical evaluation of APS algorithms.

A comparative summary of major model properties is provided in Table 1.1.

Table 1.1: Comparative overview of principal glucose–insulin model categories [1, 2].

Model	States	Physiological detail	Controller design	Clinical use
Bergman Minimal	3–4	Moderate	Very high	IVGTT analysis
Hovorka	9	High	Moderate	MPC design
Dalla Man	13	Very high	Low	Simulation
Sorensen	19	Very high	Very low	Physiological research
UVa/Padova Simulator	>20	Very high	Simulation only	FDA preclinical

1.3.2 Key Modeling Challenges

Despite the availability of numerous models, several challenges persist in mathematical modeling of the glucose–insulin system [1]:

- **Nonlinearity**: The product of glucose concentration and remote insulin action in the Bergman model, and similar bilinear couplings in other models, produce inherently nonlinear dynamics that cannot be accurately represented by linear approximations over the full operating range.
- **Parameter uncertainty**: Model parameters vary significantly between patients (inter-patient variability) and within the same patient over time (intra-patient variability) due to changes in insulin sensitivity, stress, infection, physical activity, and hormonal fluctuations [9, 10].
- **Unmodeled disturbances**: Meal absorption, physical exercise, glucagon secretion, and gastric emptying introduce disturbances that are difficult to model precisely or predict in advance [1].
- **Sensor imperfections**: CGM devices measure interstitial glucose rather than plasma glucose, introducing a physiological delay and measurement noise that degrade the quality of feedback information available to the controller [21].

1.4 Control Strategies for Blood Glucose Regulation

The design of a blood glucose controller for the artificial pancreas is an active and rapidly evolving research area. A wide spectrum of control methodologies has been investigated over the past four decades, ranging from classical linear techniques to sophisticated nonlinear

and adaptive strategies. This section provides a structured review of the most significant approaches reported in the literature.

1.4.1 Linear Control Approaches

Early APS algorithms were based on linear control theory, primarily because of its mathematical simplicity and well-established design tools.

PID control. Proportional–Integral–Derivative (PID) controllers were among the first closed-loop glucose regulation strategies proposed [22]. The control signal is a linear combination of the glucose error, its integral, and its derivative. While PID controllers are simple to implement and provide adequate performance under nominal conditions, they do not account for the nonlinear glucose–insulin dynamics, are sensitive to parameter variations, and may produce hypoglycaemic undershoot if gains are not carefully calibrated [1, 9].

H_∞ robust control. Robust H_∞ controllers were proposed to improve rejection of disturbances and parameter uncertainty by minimising the worst-case gain from disturbances to output [23]. Linear Parameter Varying (LPV) H_∞ controllers extended this approach to capture some of the scheduling effects of the nonlinear glucose dynamics [10]. However, the linearisation required to apply these methods introduces significant model error at operating points far from the nominal, limiting their reliability in the postprandial regime.

Limitations of linear controllers. As highlighted in [1, 9], linear controllers share three fundamental deficiencies when applied to the T1DM problem: (i) aggressive integral action can lead to hypoglycaemic events; (ii) linearisation of the nonlinear physiological model discards clinically relevant information about insulin sensitivity; and (iii) fixed-gain designs cannot adapt to the time-varying and patient-specific nature of the glucose–insulin system. These limitations have motivated a shift toward nonlinear and adaptive approaches.

1.4.2 Model Predictive Control

Model Predictive Control (MPC) has emerged as the dominant control paradigm for commercial APS systems. MPC solves a constrained optimisation problem at each sampling instant

to find the insulin infusion sequence that minimises predicted glucose excursions over a finite horizon, subject to physical constraints ($u \geq 0$, glucose safety bounds) [24].

MPC offers several advantages for APS applications: it explicitly handles actuator constraints, can incorporate meal announcements as feedforward disturbances, and provides a systematic framework for multi-objective optimisation. The Hovorka model [4] has been extensively used as the internal prediction model for MPC [1].

Adaptive MPC extensions update the internal model parameters online using recursive identification, allowing the controller to compensate for changing insulin sensitivity [25, 26]. Despite its commercial success, standard MPC has several limitations: it requires significant computational resources, the prediction accuracy depends critically on the internal model quality, and robust performance guarantees are difficult to establish analytically [1].

1.4.3 Sliding Mode Control

Sliding Mode Control (SMC) is a nonlinear robust control technique that drives the system state onto a designed switching surface and maintains it there, making the closed-loop behavior insensitive to matched disturbances and parameter uncertainties [27, 28]. SMC has been applied to the Bergman model and its extensions, demonstrating robustness to meal disturbances and inter-patient variability.

Higher-order sliding mode controllers (2-SMC, super-twisting) were proposed to eliminate the chattering phenomenon inherent in first-order SMC, which is clinically unacceptable because it would produce high-frequency oscillations in the insulin infusion rate [28, 10]. Terminal SMC variants provide finite-time convergence guarantees, which is advantageous for rapid correction of severe hyperglycaemia [29, 30].

The main limitation of SMC for APS applications is the requirement for precise knowledge of the system model structure and the difficulty of guaranteeing the non-negativity constraint on insulin infusion during sliding [1].

1.4.4 Backstepping Control

The backstepping methodology provides a systematic procedure for constructing Lyapunov-based controllers for nonlinear systems in strict or semi-strict feedback form [31]. The cascaded structure of the Bergman model, in which the control input reaches the glucose equa-

tion through the chain plasma insulin → remote insulin → glucose, is well suited to the backstepping approach.

Adaptive backstepping controllers for blood glucose regulation have been proposed in several works [31, 32, 33, 34], demonstrating improved robustness to parameter uncertainty compared to non-adaptive nonlinear methods. Integral backstepping further improves steady-state tracking accuracy. The dynamical backstepping (DBST) approach of [10] provided rigorous stability analysis and demonstrated robustness to insulin pump faults.

The primary drawback of backstepping is its computational complexity: the recursive differentiation of virtual control laws generates increasingly complex expressions, and the resulting controller is difficult to implement in resource-constrained embedded systems.

1.4.5 Feedback Linearisation

Feedback linearisation transforms the nonlinear glucose–insulin dynamics into a linear system by cancelling the nonlinear terms through a state-dependent input transformation. Input–output feedback linearisation has been applied to the Bergman model and its extensions [35, 10], yielding controllers that are globally stabilising under exact model knowledge.

However, feedback linearisation is inherently sensitive to model errors: parameter uncertainty or unmodelled dynamics cause residual nonlinearities that degrade performance and can destabilise the closed-loop system. Robust extensions combining feedback linearisation with disturbance observers have been proposed to mitigate this sensitivity [1].

1.4.6 Synergetic Control

Synergetic control, closely related to SMC but producing a continuous control law, forces the system to evolve on a designer-specified macro-variable manifold through an exponential convergence law. It inherits the robustness properties of SMC while eliminating chattering [29]. Terminal synergetic control combines this approach with terminal attractor techniques to achieve finite-time convergence to the normoglycaemic setpoint, which is particularly valuable for the rapid correction of postprandial hyperglycaemia [29, 30].

1.4.7 Fuzzy Logic and Neural Network-Based Control

Fuzzy logic controllers represent expert clinical knowledge as if-then rules and have been applied to blood glucose regulation with promising simulation results [36]. Artificial neural network (ANN) controllers learn the input-output mapping from patient data and can capture complex nonlinear behaviors without an explicit model [37]. Reinforcement learning-based controllers have also been explored as a means of personalising the control policy through online interaction with the patient's glucose response [38].

The principal limitation of data-driven methods is the lack of formal stability and safety guarantees, which are essential requirements for medical devices.

1.4.8 Adaptive Control

Adaptive controllers continuously adjust their parameters or gains in response to changing plant conditions, making them intrinsically suited to the time-varying and patient-specific nature of the glucose–insulin system.

Model Reference Adaptive Control (MRAC). MRAC drives the plant output to track a reference model output through an online gain adaptation law derived from a Lyapunov stability analysis. Several MRAC schemes have been proposed for blood glucose regulation using both the Bergman model and the Hovorka model [9, 39]. The adaptive parametric compensation approach of [9] demonstrated that MRAC could compensate for $\pm 30\%$ parameter uncertainty while avoiding hypoglycaemic events in a population of 200 virtual T1DM patients.

Self-tuning and indirect adaptive control. Minimum variance controllers, self-tuning regulators, and adaptive LQG schemes combined with Kalman filter or recursive least-squares parameter estimation have also been explored [9]. These indirect approaches require online system identification, which may be unreliable when excitation is insufficient.

Table 1.2 summarises the key characteristics of the major control strategies reviewed above.

Table 1.2: Comparative summary of control strategies for blood glucose regulation in T1DM [1].

Strategy	**Model-based**	**Adaptive**	**Stability proof**	**Finite-time**	**Complexity**
PID	Partial	No	No	No	Low
H_∞/LPV	Yes	No	Yes	No	Medium
MPC	Yes	Partial	Limited	Partial	High
SMC / HOSMC	Yes	Yes	Yes	Yes	Medium
Backstepping	Yes	Yes	Yes	Yes	High
Feedback Lin.	Yes	No	Yes	No	Medium
Synergetic	Yes	Yes	Yes	Yes	Medium
MRAC / SAC	Yes	Yes	Yes	No	Low–Medium
Fuzzy / ANN	No	Yes	Limited	No	Medium

1.5 Open Challenges in Artificial Pancreas Control

Despite four decades of research and the recent commercial availability of hybrid closed-loop systems, several fundamental challenges remain unsolved and constitute active areas of investigation [1, 17]:

1.5.1 Inter- and Intra-Patient Variability

Physiological parameters governing glucose–insulin dynamics, particularly insulin sensitivity (p_3/p_2 in the Bergman model), insulin clearance rate (p_4), and meal absorption characteristics — vary by up to $\pm 30\%$ between patients and change within the same patient due to stress, illness, hormonal cycles, and physical activity [9, 10]. A control strategy designed for nominal parameters may deliver insufficient insulin to an insulin-resistant patient or dangerously high insulin to a highly sensitive one. The design of controllers that are robustly stable and performant across the full physiological range of human variability is a central open problem.

1.5.2 Unannounced Meal Disturbances

Meal ingestion is the dominant disturbance in glucose regulation and can raise blood glucose by 100–200 mg/dL within 30–60 min. While meal-announcement schemes (carbohydrate counting) are available, they are imprecise and require patient effort. Fully automated APS systems must detect and reject meal disturbances without prior knowledge, which demands

disturbance observers or sufficiently robust control laws [1, 40].

1.5.3 Exercise and Counter-Regulatory Hormones

Physical exercise increases peripheral glucose uptake and can trigger counter-regulatory hormone secretion (glucagon, epinephrine, cortisol), causing complex and patient-specific glucose excursions that are difficult to model. Current APS systems handle exercise poorly, often resulting in delayed hypoglycaemia during or after activity [41, 42].

1.5.4 Sensor Noise and CGM Delays

Continuous glucose monitors measure interstitial glucose, which lags behind plasma glucose by 5–15 min during rapid glucose changes. Additionally, CGM signals are corrupted by sensor noise and drift, and occasional large errors or signal dropouts occur due to compression artefacts or calibration errors [21]. Control algorithms must be robust to these sensor imperfections while remaining responsive to genuine glucose excursions.

1.5.5 Stability and Safety Guarantees

Many high-performing control approaches, particularly those based on machine learning and neural networks, lack formal closed-loop stability guarantees and mathematically provable safety properties. For a medical device that operates continuously in a life-critical environment, the existence of rigorous stability proofs and analytically verified safety constraints (no hypoglycaemia, bounded insulin delivery) is an essential requirement that many current approaches do not fully satisfy [1, 43].

1.5.6 Computational Constraints and Wearability

APS devices must operate on battery-powered wearable hardware with limited computational resources. Complex optimisation-based methods such as nonlinear MPC require significant processing power and may be unsuitable for low-power embedded implementations. The development of control algorithms with low computational footprint and guaranteed real-time execution is therefore an important practical constraint [1].

1.5.7 Personalisation and Long-Term Adaptation

Insulin sensitivity and other physiological parameters change gradually over time due to disease progression, weight changes, seasonal variations, and aging. An APS must continuously adapt its behaviour to reflect these long-term changes without requiring manual recalibration by a clinician. Online parameter adaptation with formal convergence guarantees remains an open research problem [25, 26].

1.6 Proposed Approach and Contribution of This Thesis

The preceding review reveals a persistent gap in the existing literature: the most theoretically rigorous adaptive control methods (MRAC, backstepping) require knowledge of the plant model structure and either full-state feedback or complex state observers, while the simplest methods (PID, MPC) lack formal stability guarantees or adequate robustness to parametric uncertainty.

This thesis proposes the application of **Simple Adaptive Control** (SAC) [44, 45, 46] to the blood glucose regulation problem in T1DM. SAC is a direct Model Reference Adaptive Control strategy that adapts a gain matrix in real time based solely on the measurable output error between the plant and a reference model, without requiring a plant identifier, a state observer, or explicit knowledge of the plant parameters.

The proposed approach addresses the key challenges identified in Section 1.5 in the following ways:

- **Robustness to parameter variability**: The adaptive gain mechanism automatically compensates for inter-patient and intra-patient parameter variations by updating gains in response to the observed tracking error, without requiring explicit knowledge of the patient's physiological parameters.
- **Formal stability guarantees**: The SAC stability theory, based on the concept of Almost Strict Passivity (ASP) for nonlinear systems [44, 46], provides rigorous Lyapunov-based proofs that all closed-loop signals remain bounded and that tracking error converges to zero.

- **Low computational complexity**: The SAC control law requires only standard matrix multiplications and first-order differential equations for gain adaptation, making it suitable for embedded real-time implementation.
- **No state observer required**: The entire adaptation mechanism operates on the scalar output tracking error $e_y(t) = G_b - G(t)$, which is directly available from the CGM measurement.
- **Meal disturbance rejection**: The extended four-state Bergman model [19, 9] used as the plant explicitly includes meal dynamics as a fourth state, and the adaptive gains adjust in real time to compensate for postprandial glucose excursions.

The specific mathematical plant adopted is the extended Bergman Minimal Model [6, 19, 9], consisting of four coupled nonlinear differential equations describing plasma glucose, remote insulin effect, plasma insulin concentration, and meal disturbance rate. This model belongs to the class of nonlinear systems linear in control, which is precisely the class for which the SAC stability theory of [44] provides rigorous guarantees.

The controller is evaluated through a two-part simulation benchmark: (i) Test 1 assesses robustness to inter-patient variability across ten virtual patients with ±30% parameter uncertainty; (ii) Test 2 evaluates tracking performance across ten clinical scenarios spanning normal fasting to critical hyperglycaemia; and (iii) Test 3 validates the controller under a realistic full-day protocol with three meals.

1.7 Thesis Structure

The remainder of this thesis is organised as follows.

Chapter 2 — Mathematical Modeling of the Glucose–Insulin System presents the mathematical foundations of glucose–insulin modeling. The fundamental principles of physiological modeling (mass balance, compartmental representation, state-space formulation) are introduced and a comparative review of existing model categories is provided. The extended Bergman Minimal Model is then derived in detail, with each equation analysed in physiological and mathematical terms. The chapter concludes with the complete four-state state-space representation and a discussion of parameter significance and inter-patient variability.

Chapter 3 — Simple Adaptive Control of the Bergman Minimal Model constitutes the core technical contribution of the thesis. The SAC algorithm is introduced within the

passivity-based framework of [44], and the key theoretical tools, strict passivity, almost strict passivity, and the parallel feedforward compensator lemma, are stated and proved for the class of nonlinear systems considered. The application of SAC to the Bergman model is derived analytically, and a Lyapunov-based stability theorem establishing the robust adaptive stability of the closed-loop system is presented with a complete proof. The chapter concludes with the three-part simulation study and a detailed discussion of results.

General Conclusion summarises the principal contributions of the thesis, discusses the limitations of the proposed approach, and identifies directions for future work, including experimental validation on CGM data and extension to multi-hormone (insulin + glucagon) APS architectures.

Chapter Summary

This chapter has established the clinical, physiological, and engineering context motivating the research presented in this thesis. Type 1 Diabetes Mellitus, characterised by the autoimmune destruction of pancreatic β-cells and the resulting absence of endogenous insulin secretion, requires permanent exogenous insulin therapy and continuous blood glucose monitoring. The artificial pancreas system, which automates this therapy through a closed-loop control algorithm, has been the subject of intensive research for over four decades. A comprehensive review of mathematical modeling approaches and control strategies, from classical PID and robust H_∞ methods through model predictive control, sliding mode, backstepping, feedback linearisation, synergetic, and adaptive techniques, identified the key open challenges: inter-patient variability, unannounced meal disturbances, sensor noise, and the need for formal stability guarantees with low computational overhead. These challenges motivate the Simple Adaptive Control approach developed in this thesis, which combines formal passivity-based stability guarantees with real-time gain adaptation requiring no plant parameter knowledge.

Chapter 2

Mathematical Modeling of the Glucose–Insulin System

2.1 Introduction

The development of Artificial Pancreas Systems (APS) relies fundamentally on the availability of mathematical models capable of accurately describing the physiological mechanisms governing glucose–insulin regulation. Mathematical modeling provides a quantitative framework through which biological processes can be analysed, simulated, predicted, and controlled. In the context of Type 1 Diabetes Mellitus (T1DM), models play a central role in understanding glucose metabolism, evaluating therapeutic strategies, designing control algorithms, and conducting safe in silico experiments prior to clinical implementation [2, 3, 47].

Unlike healthy individuals, patients with T1DM exhibit impaired endogenous insulin secretion due to autoimmune destruction of pancreatic β-cells. Consequently, maintaining blood glucose concentrations within a physiological range requires external insulin administration and continuous monitoring. The complexity of this regulation process arises from the nonlinear interactions between glucose absorption, insulin kinetics, insulin action, hepatic glucose production, peripheral glucose utilization, hormonal fluctuations, and meal disturbances. Mathematical models provide a systematic means of representing these interactions and form the foundation upon which advanced control strategies are developed.

This chapter presents the mathematical foundations of glucose–insulin modeling as a prerequisite to the controller design developed in Chapter 3. The chapter begins with a brief overview of physiological modeling principles and a comparative review of existing glucose–insulin models. This comparative analysis is then used to motivate and justify the adoption of the extended Bergman Minimal Model as the mathematical plant for the adaptive controller developed in this thesis. The remainder of the chapter derives the complete four-state model, analyses each equation in physiological and mathematical terms, and arrives at the

state-space representation that is carried forward into the control design of Chapter 3.

2.2 Principles of Physiological Modeling

Physiological modeling seeks to represent biological systems through mathematical relationships that describe dynamic interactions among physiological variables. The development of such models generally follows three fundamental principles: conservation laws, compartmental representation, and dynamic system theory.

2.2.1 Mass Balance and Conservation Laws

Conservation laws form the basis of most physiological models and ensure that mass balances are respected. For glucose metabolism, the rate of change of blood glucose concentration can be expressed as the difference between glucose appearance and glucose disappearance:

$$\frac{dG(t)}{dt} = R_a(t) + EGP(t) - U_g(t) - E(t), \tag{2.1}$$

where $G(t)$ is blood glucose concentration [mg/dL], $R_a(t)$ is the rate of glucose appearance from meals [mg/dL/min], $EGP(t)$ is endogenous (hepatic) glucose production [mg/dL/min], $U_g(t)$ is glucose utilization by tissues [mg/dL/min], and $E(t)$ is renal glucose excretion [mg/dL/min]. Equation (2.1) represents the fundamental mass balance governing glucose metabolism and underpins most physiological and control-oriented models.

2.2.2 Compartmental Modeling

Compartmental modeling divides biological systems into interconnected subsystems that exchange substances according to predefined transfer mechanisms. Each compartment represents a physiological region, tissue, or functional subsystem in which the modeled substance is assumed to be uniformly distributed. The dynamic evolution of the quantity stored in compartment i obeys the general balance:

$$\frac{dx_i(t)}{dt} = \sum q_{\text{in}}(t) - \sum q_{\text{out}}(t), \tag{2.2}$$

where q_{in} and q_{out} represent the inflow and outflow rates. The compartmental approach has become the dominant modeling methodology in diabetes research due to its physiological interpretability and compatibility with control-oriented analysis.

2.2.3 State-Space Representation

Control engineering applications require models to be expressed in state-space form. A general nonlinear physiological model can be written as:

$$\dot{x}(t) = f(x(t),\, u(t),\, d(t))\,, \tag{2.3}$$

$$y(t) = h(x(t))\,, \tag{2.4}$$

where $x(t) \in \mathbb{R}^n$ is the state vector, $u(t)$ is the control input (insulin infusion rate), $d(t)$ represents external disturbances (meals, physical activity), and $y(t)$ is the measurable output (glucose concentration). State-space formulations constitute the mathematical framework upon which adaptive controllers such as those developed in Chapter 3 are designed.

2.3 Overview of Glucose–Insulin Models

Over the past four decades, numerous mathematical models of glucose–insulin metabolism have been proposed in the literature. These models differ significantly in complexity, physiological detail, computational requirements, and intended applications. Understanding their respective strengths and limitations is essential for selecting an appropriate model for artificial pancreas controller design.

2.3.1 Physiological Models

Physiological models aim to represent biological mechanisms with high anatomical and biochemical fidelity. They typically contain numerous compartments and parameters corresponding to specific organs and metabolic pathways.

The **Sorensen model** (1985) is among the most representative examples of this category [3]. It includes detailed descriptions of glucose, insulin, and glucagon transport among multiple organ compartments, including the liver, kidneys, brain, muscle tissue, and adipose tissue. The model accurately reproduces a wide range of metabolic responses under varying

physiological conditions. However, its large number of state variables and parameters makes parameter identification difficult and limits its applicability to real-time control design.

The **Dalla Man model** (2007) [20] extends the compartmental approach by incorporating detailed meal absorption pharmacokinetics, subcutaneous insulin delivery, and a comprehensive description of hepatic glucose regulation. While it provides excellent predictive accuracy in postprandial conditions, its complexity is prohibitive for direct use in analytical controller synthesis.

2.3.2 Simulator-Based Models

Population-based simulators extend physiological models by incorporating inter-patient variability. The **UVa/Padova Type 1 Diabetes Simulator** [5], accepted by the U.S. Food and Drug Administration (FDA) as a substitute for preclinical animal testing, is the most widely used tool of this type. It represents a cohort of 30 virtual subjects (adults, adolescents, and children) characterised by distinct physiological parameters, enabling rigorous statistical evaluation of closed-loop control algorithms. However, the simulator's internal model is not intended for analytical controller design.

2.3.3 Control-Oriented Models

Control-oriented models are specifically designed for controller synthesis, stability analysis, and real-time implementation. Their structure prioritizes mathematical tractability and dynamic accuracy over exhaustive physiological representation.

The **Hovorka model** [4] describes subcutaneous insulin absorption, insulin kinetics, insulin action on glucose transport, and glucose distribution through a system of interconnected compartments. It has been widely used in model predictive control (MPC) studies, particularly in commercial closed-loop devices. The model's moderate complexity makes it suitable for optimization-based controllers but introduces significant computational overhead for real-time adaptive schemes.

The **Bergman Minimal Model** [48, 6] is the simplest and most widely studied control-oriented model. Its parsimonious structure captures the dominant glucose–insulin dynamics through a compact system of differential equations while preserving full physiological interpretability. Extensions of the model that incorporate meal dynamics and insulin pump kinetics have been proposed in the literature [19, 9] and retain the computational simplicity

essential for adaptive control applications.

Table 2.1 provides a comparative summary of the major model categories.

Table 2.1: Comparative summary of glucose–insulin model categories [2, 3, 4, 5, 6].

Model	**Complexity**	**Physiological detail**	**Control suitability**	**Identification**
Sorensen	Very high	Very high	Low	Difficult
Dalla Man	High	High	Low	Moderate
UVa/Padova	Very high	High	Simulation only	N/A
Hovorka	Moderate	Moderate	Moderate	Moderate
Bergman Minimal	Low	Moderate	Very high	Easy

2.3.4 Justification for the Bergman Minimal Model

The selection of a mathematical plant model is a critical design decision that directly influences the complexity, stability guarantees, and implementability of the resulting controller. For the Simple Adaptive Control (SAC) framework developed in Chapter 3, the plant model must satisfy three requirements simultaneously:

1. It must be expressible in the nonlinear state-space form $\dot{x}_p = A_p(x_p)x_p + B_p u$ required by the passivity-based SAC stability theory of [44].

2. It must be sufficiently simple to support analytical passivity verification and closed-form controller derivation.

3. It must faithfully represent the dominant glucose–insulin dynamics, including meal disturbances and the delay in insulin action.

The extended Bergman Minimal Model satisfies all three requirements and is therefore adopted as the plant model throughout this thesis. Its nonlinear state matrix $A_p(x_p)$ depends only on the glucose concentration x_1 and the remote insulin effect x_2, both of which are physiologically bounded, ensuring that the uniform boundedness assumption required by the SAC theory is satisfied [44, 46]. Its low dimension (four states) makes parameter identification straightforward from standard clinical measurements. Finally, the Fisher meal extension [19] and the explicit insulin pump dynamics included in the formulation of [9] provide sufficient physiological realism for realistic simulation studies.

Highly detailed models such as those of Sorensen, Dalla Man, or the UVa/Padova simulator, while valuable for physiological research and population-level validation, are unnecessarily complex for analytical controller design and would obscure the stability analysis presented in Chapter 3.

2.4 The Bergman Minimal Model: Historical Background

The origins of the Bergman Minimal Model can be traced to the late 1970s, when researchers sought reliable methods for quantifying insulin sensitivity in humans. At that time, experimental techniques were capable of measuring plasma glucose and insulin concentrations during metabolic tests, but no practical mathematical framework existed to extract meaningful physiological information from these measurements.

To address this problem, Bergman, Phillips, and Cobelli introduced a mathematical model capable of interpreting data obtained from the *Intravenous Glucose Tolerance Test* (IVGTT) [48, 6]. Their objective was not to reproduce every physiological detail of glucose metabolism but rather to develop the simplest model capable of explaining the observed glucose response following an intravenous glucose bolus.

This philosophy led to the concept of a *minimal model*: a mathematical representation containing the minimum number of state variables and parameters required to reproduce experimentally observed dynamics while preserving physiological meaning. The resulting model provided, for the first time, a quantitative framework for estimating insulin sensitivity from clinical data and demonstrated that relatively simple mathematical structures could successfully describe complex physiological processes.

2.4.1 The Intravenous Glucose Tolerance Test

During an IVGTT experiment, a predetermined quantity of glucose is injected directly into the bloodstream at time $t = 0$. Plasma glucose and insulin concentrations are then measured periodically over several hours. The typical sequence of physiological events is as follows, as illustrated in figure 2.1:

1. Intravenous glucose administration produces a rapid rise in plasma glucose concentra-

tion above its fasting basal level G_b.

2. Pancreatic β-cells detect hyperglycaemia and secrete insulin into the bloodstream.

3. Elevated plasma insulin activates glucose uptake mechanisms in peripheral tissues and suppresses hepatic glucose production.

4. Plasma glucose progressively returns toward the basal level G_b.

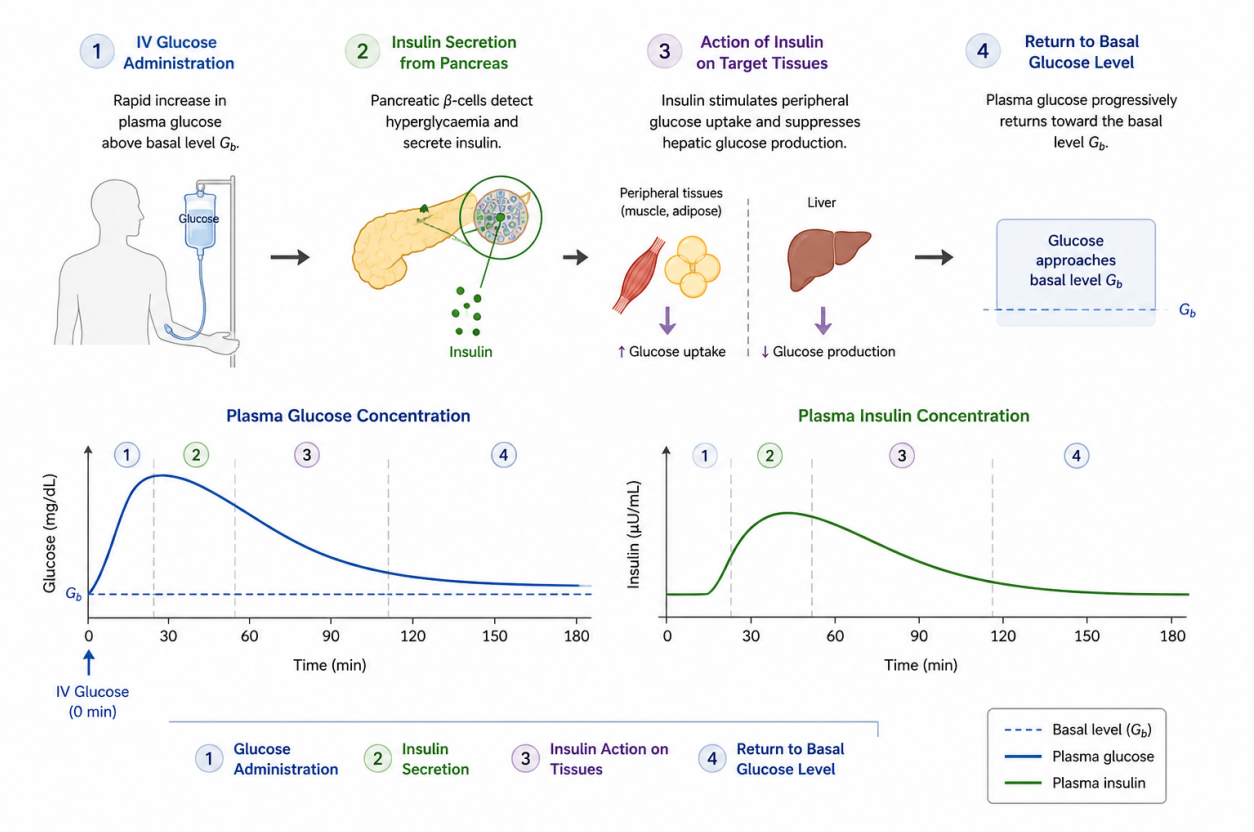

Figure 2.1: IVGTT experiment sequence diagram

A key experimental observation during IVGTT studies was that, although plasma insulin concentration changes rapidly following glucose administration, the metabolic effect of insulin on glucose disposal does not occur instantaneously. A measurable time delay exists between insulin appearance in the bloodstream and its action on target tissues. This observation motivated Bergman to introduce the concept of a *remote insulin compartment*, one of the defining features of the Minimal Model.

2.5 The Three-State Bergman Minimal Model

The original Bergman Minimal Model describes glucose–insulin dynamics through three coupled state variables:

1. $G(t)$: plasma glucose concentration [mg/dL],
2. $X(t)$: remote insulin action [min^{-1}],
3. $I(t)$: plasma insulin concentration [mU/L].

2.5.1 Glucose Dynamics

The first equation describes the temporal evolution of plasma glucose concentration. The model assumes that glucose decreases through two mechanisms: insulin-independent uptake (governed by glucose effectiveness) and insulin-dependent uptake (governed by remote insulin action):

$$\frac{dG(t)}{dt} = -\big[p_1 + X(t)\big]\, G(t) + p_1\, G_b, \tag{2.5}$$

where p_1 [min^{-1}] is the *glucose effectiveness* coefficient and G_b [mg/dL] is the basal glucose concentration.

The term $p_1\, G_b$ represents the natural tendency of the organism to maintain glucose near its basal equilibrium level, reflecting hepatic glucose production and insulin-independent tissue uptake. The term $-[p_1 + X(t)]\, G(t)$ represents total glucose disposal, where $X(t)$ quantifies the additional contribution of insulin action. Equation (2.5) can be rewritten equivalently as:

$$\frac{dG(t)}{dt} = -p_1\big(G(t) - G_b\big) - X(t)\, G(t), \tag{2.6}$$

which makes the self-restoring nature of the p_1 term more explicit: when $G(t) > G_b$ the first term is negative (glucose is driven down), and when $G(t) < G_b$ it becomes positive (hepatic glucose production prevents further decline).

2.5.2 Remote Insulin Action Dynamics

One of the most innovative aspects of the Bergman model is the introduction of the auxiliary state $X(t)$, which represents the cumulative, delayed action of insulin on peripheral glucose

disposal. Rather than a physical compartment, $X(t)$ is a functional variable that captures the lag between insulin appearance in plasma and its metabolic effects on target tissues:

$$\frac{dX(t)}{dt} = -p_2\, X(t) + p_3\big(I(t) - I_b\big), \tag{2.7}$$

where p_2 [min^{-1}] is the insulin action decay rate, p_3 [$\mu\mathrm{U\,mL}^{-1}\,\mathrm{min}^{-2}$] is the insulin sensitivity parameter, $I(t)$ [mU/L] is the plasma insulin concentration, and I_b [mU/L] is the basal insulin concentration.

The parameter p_2 determines the rate at which insulin action dissipates once plasma insulin returns to its basal level; its reciprocal $1/p_2$ [min] defines the time constant of remote insulin action (approximately 67 min at nominal values). The parameter p_3 quantifies the ability of supra-basal plasma insulin to activate glucose disposal mechanisms: patients with insulin resistance present lower values of p_3, while highly insulin-sensitive individuals present higher values.

When plasma insulin exceeds the basal level ($I > I_b$), $X(t)$ increases, accelerating glucose removal from the bloodstream. Conversely, when $I = I_b$, remote insulin action decays exponentially to zero, and glucose dynamics revert to insulin-independent behavior.

2.5.3 Plasma Insulin Dynamics

The third state equation governs the dynamics of plasma insulin concentration. In the original IVGTT formulation, plasma insulin is an exogenous input driven by pancreatic secretion stimulated by hyperglycaemia. In the T1DM closed-loop context, where endogenous secretion is absent, insulin dynamics are governed entirely by exogenous delivery and clearance:

$$\frac{dI(t)}{dt} = -p_4\big(I(t) - I_b\big) + u(t), \tag{2.8}$$

where p_4 [min^{-1}] is the plasma insulin clearance rate (with time constant $1/p_4 \approx 5$ min at nominal values) and $u(t)$ [mU/min] is the exogenous insulin infusion rate delivered by the insulin pump.

When $u(t) = 0$ and $I(t) > I_b$, plasma insulin decays exponentially toward the basal level with time constant $1/p_4$. The rapid clearance dynamics of plasma insulin ($p_4 = 0.2$ min^{-1}) contrast with the much slower remote insulin dynamics ($p_2 = 0.015$ min^{-1}), capturing the well-known lag between plasma insulin and its metabolic action.

2.5.4 Equilibrium Analysis

The equilibrium of the three-state model is reached when all time derivatives vanish simultaneously. Setting $\dot{G} = \dot{X} = \dot{I} = 0$ and $u = 0$ gives the unique basal equilibrium:

$$G^* = G_b, \quad X^* = 0, \quad I^* = I_b. \tag{2.9}$$

This equilibrium is physiologically meaningful: at basal conditions there is no net remote insulin action ($X^* = 0$), plasma insulin is at its fasting level ($I^* = I_b$), and glucose is at its setpoint ($G^* = G_b$). The artificial pancreas controller must drive the system to this equilibrium from an arbitrary hyperglycaemic initial condition.

2.6 Extension to the Four-State Model with Meal Dynamics

The three-state model described in Section 2.5 was derived from IVGTT experiments in which meal disturbances are absent. In a closed-loop artificial pancreas setting, however, meal ingestion constitutes the primary disturbance input and must be included in the model to ensure realistic evaluation of controller performance.

Fisher [19] proposed representing the meal disturbance as a fourth state variable whose dynamics describe the rate of glucose appearance in the plasma compartment following food intake. This extension, adopted by [9, 29, 8], preserves the mathematical structure of the Bergman model while providing a physiologically consistent description of postprandial glucose excursions.

2.6.1 Meal Disturbance Dynamics

The meal disturbance state $D(t)$ [mg/dL/min] represents the rate of glucose appearance in the plasma resulting from food absorption. Its dynamics are modeled as a first-order decay process:

$$\frac{dD(t)}{dt} = -p_5\, D(t), \tag{2.10}$$

where p_5 [min^{-1}] is the meal absorption decay rate. At the onset of a meal event, $D(t)$ is instantaneously incremented by the meal amplitude D_0 [mg/dL/min], which reflects the car-

bohydrate content and absorption rate of the meal. Subsequently, $D(t)$ decays exponentially toward zero with time constant $1/p_5 \approx 20$ min, representing the progressive gastric emptying and intestinal absorption of ingested glucose.

The total glucose load delivered to the plasma by a single meal event is:

$$\int_0^\infty D(t)\,dt = \frac{D_0}{p_5}, \tag{2.11}$$

which is directly proportional to the carbohydrate content. Standard meal amplitudes used in simulation studies are in the range $D_0 \in [3, 10]$ mg/dL/min, corresponding to light snacks through heavy meals [9, 29].

2.6.2 Extended Glucose Dynamics

The glucose dynamics equation (2.6) is augmented with the meal disturbance term:

$$\frac{dG(t)}{dt} = -p_1\big(G(t) - G_b\big) - X(t)\,G(t) + D(t). \tag{2.12}$$

The new term $D(t)$ acts as a positive-valued input disturbance that temporarily elevates glucose above its basal level following a meal, challenging the controller to restore normoglycaemia.

2.7 Complete Four-State Model

Combining the extended glucose equation (2.12) with the remote insulin equation (2.7), the plasma insulin equation (2.8), and the meal dynamics equation (2.10), the complete four-state extended Bergman Minimal Model adopted in this thesis is:

$$\frac{dG(t)}{dt} = -p_1\big(G(t) - G_b\big) - X(t)\,G(t) + D(t), \tag{2.13}$$

$$\frac{dX(t)}{dt} = -p_2\,X(t) + p_3\big(I(t) - I_b\big), \tag{2.14}$$

$$\frac{dI(t)}{dt} = -p_4\big(I(t) - I_b\big) + u(t), \tag{2.15}$$

$$\frac{dD(t)}{dt} = -p_5\,D(t), \tag{2.16}$$

with the measurable output:

$$y(t) = G(t). \tag{2.17}$$

The four state variables and their physical meanings are:

- $G(t)$ [mg/dL]: plasma (blood) glucose concentration — the primary regulated variable and the only directly measurable state in clinical practice (via continuous glucose monitoring);
- $X(t)$ [min^{-1}]: remote insulin effect — a functional variable representing the delayed, cumulative action of plasma insulin on peripheral glucose disposal;
- $I(t)$ [mU/L]: plasma insulin concentration — determined by exogenous infusion $u(t)$ and first-order clearance;
- $D(t)$ [mg/dL/min]: meal glucose disturbance rate — represents the rate of glucose appearance in plasma from food absorption.

The control input $u(t)$ [mU/min] is the exogenous insulin infusion rate delivered by the insulin pump and is the only degree of freedom available to the artificial pancreas controller. It is constrained to be non-negative at all times ($u(t) \geq 0$) since an insulin pump can only deliver insulin and cannot withdraw it from the bloodstream.

2.7.1 Parameter Summary

The complete set of model parameters, their units, nominal values, and physiological meanings are summarised in Table 2.2.

2.7.2 Inter-Patient Variability

A fundamental challenge in artificial pancreas design is that model parameters vary considerably from one patient to another. Important physiological factors such as insulin sensitivity (p_3/p_2), insulin clearance (p_4), and meal absorption (p_5) exhibit significant inter-patient variability. Published studies report variability ranges of $\pm 30\%$ on p_2, p_3, and p_4, and $\pm 10\%$ on p_5 around nominal values [9, 10]. Additionally, intra-patient variability due to stress, physical activity, and hormonal fluctuations further complicates real-time regulation.

Table 2.2: Parameters of the extended Bergman Minimal Model. Nominal values from [7, 8, 9].

Parameter	Unit	Nominal value	Physiological meaning
p_1	min^{-1}	0.028	Glucose effectiveness: insulin-independent glucose uptake and hepatic self-regulation
p_2	min^{-1}	0.015	Remote-insulin decay rate (time constant $\approx$ 67 min)
p_3	$\mu\mathrm{U\,mL^{-1}\,min^{-2}}$	2.0×10^{-6}	Insulin sensitivity: gain from plasma insulin to remote insulin action
p_4	min^{-1}	0.200	Plasma insulin clearance rate (time constant $\approx$ 5 min)
p_5	min^{-1}	0.050	Meal disturbance decay rate (time constant $\approx$ 20 min)
G_b	$\mathrm{mg\,dL^{-1}}$	80	Basal plasma glucose (regulation setpoint)
I_b	$\mathrm{mU\,L^{-1}}$	7	Basal plasma insulin
$u(t)$	$\mathrm{mU\,min^{-1}}$	$\in [0, 80]$	Exogenous insulin infusion rate (control input)
$D(t)$	$\mathrm{mg\,dL^{-1}\,min^{-1}}$	$D_0 \in [3, 10]$	Meal glucose disturbance (initial amplitude per meal event)

This parametric uncertainty is one of the primary motivations for the adaptive control approach developed in Chapter 3: a controller that adapts its gains in real time can compensate for both inter-patient and intra-patient parameter variations without requiring explicit knowledge of the patient's physiological parameters.

2.8 State-Space Formulation

For the purpose of controller design, it is convenient to collect the four state variables into a single state vector:

$$x_p(t) = \big[x_1(t),\ x_2(t),\ x_3(t),\ x_4(t)\big]^{\mathsf{T}} = \big[G(t),\ X(t),\ I(t),\ D(t)\big]^{\mathsf{T}}, \tag{2.18}$$

so that the model (2.13)–(2.17) can be written in the compact nonlinear state-space form of (2.3):

$$\dot{x}_p(t) = A_p(x_p)\,x_p(t) + B_p\,u(t), \qquad y(t) = C_p\,x_p(t), \tag{2.19}$$

with:

$$A_p(x_p) = \begin{bmatrix} -(p_1 + x_2) & -x_1 & 0 & 1 \\ 0 & -p_2 & p_3 & 0 \\ 0 & 0 & -p_4 & 0 \\ 0 & 0 & 0 & -p_5 \end{bmatrix}, \quad B_p = \begin{bmatrix} 0 \\ 0 \\ 1 \\ 0 \end{bmatrix}, \quad C_p = \begin{bmatrix} 1 & 0 & 0 & 0 \end{bmatrix}. \tag{2.20}$$

This representation belongs to the class of nonlinear systems linear in control of the form studied in the SAC stability theory of [44, 46]. Three structural properties of (2.19) are particularly relevant for the controller design presented in Chapter 3:

1. **Nonlinearity through** $A_p(x_p)$: The system matrix depends on the states $x_1 = G$ and $x_2 = X$ through the bilinear product $x_2 \cdot x_1$ in the glucose equation (2.13). This is the dominant nonlinearity of the model. The matrices B_p and C_p are constant, so the nonlinearity enters only through the state matrix.

2. **Uniform boundedness**: Since glucose $x_1(t)$ and remote insulin $x_2(t)$ are physiologically bounded quantities (glucose remains within $[0, 400]$ mg/dL and remote insulin within $[0, 0.1]$ min^{-1} under all clinical conditions), the matrix $A_p(x_p)$ is uniformly bounded. This property is a prerequisite for the stability theorem of the SAC algorithm [44].

3. **Cascaded structure**: The meal disturbance state $x_4 = D(t)$ evolves independently of the other states (Equation (2.16)). The control input $u(t)$ enters only through the third state $x_3 = I(t)$, and its effect propagates through $x_3 \to x_2 \to x_1$ (plasma insulin $\to$ remote insulin $\to$ plasma glucose). This three-step cascade gives the system a relative degree of three with respect to the output $y = x_1$.

2.9 Physiological Significance of the Model Parameters

A thorough understanding of the model parameters is essential both for interpreting simulation results and for assessing controller robustness. This section discusses the physiological significance of each parameter and its effect on glucose–insulin dynamics.

2.9.1 Glucose Effectiveness p_1

The parameter p_1 quantifies *glucose effectiveness* (also denoted S_G in the metabolic literature), defined as the ability of glucose itself to promote its own utilization and suppress hepatic glucose production, independently of any insulin action. This phenomenon reflects basal metabolic processes that remain active even when insulin concentration is at its basal level.

From a control standpoint, p_1 provides the only self-correcting force in the glucose equation (2.13): when $G > G_b$, the term $-p_1(G - G_b)$ is negative and drives glucose toward the setpoint; when $G < G_b$, it becomes positive, representing hepatic glucose production that prevents further decline. This term is therefore physiologically essential for closed-loop convergence: setting $p_1 \approx 0$ (as would be appropriate only for extreme T1DM cases with no residual hepatic regulation) eliminates this restoring force and leads to persistent hypoglycaemia that no insulin-only controller can correct [7]. Based on the clinical literature, the nominal value $p_1 = 0.028$ min^{-1} adopted in this thesis corresponds to typical glucose effectiveness measured in adult subjects [8].

2.9.2 Insulin Sensitivity Parameters p_2 and p_3

The parameters p_2 and p_3 jointly govern the remote insulin dynamics (2.7) and together determine the *insulin sensitivity index* (ISI), commonly defined as:

$$\text{ISI} = \frac{p_3}{p_2}. \tag{2.21}$$

A high value of p_3/p_2 indicates that a given increment in plasma insulin produces a large and sustained increase in remote insulin action, corresponding to high insulin sensitivity. Conversely, a low ratio indicates insulin resistance, where the metabolic response to insulin is attenuated.

The parameter p_2 alone determines the time constant of remote insulin dynamics ($\tau_X = 1/p_2 \approx 67$ min at nominal values), which governs the rate at which insulin's metabolic effects dissipate after plasma insulin returns to its basal level. Large values of p_2 imply rapid decay (short-acting insulin effect), while small values imply persistent remote action.

2.9.3 Plasma Insulin Clearance p_4

The parameter p_4 characterizes the rate at which the body clears insulin from the plasma compartment. Its nominal value of 0.2 min^{-1} gives a time constant of approximately 5 min, meaning that after the insulin infusion stops, plasma insulin returns to I_b within approximately 25 min (five time constants). Patients with faster clearance (higher p_4) require a higher insulin infusion rate to maintain a given plasma concentration, while patients with slower clearance (lower p_4) are more susceptible to insulin accumulation and hypoglycaemia.

2.9.4 Meal Absorption Rate p_5

The parameter p_5 determines how rapidly a meal disturbance decays once initiated. At the nominal value of 0.05 min^{-1} (time constant ≈ 20 min), a meal-induced glucose disturbance decays to less than 5% of its initial value within approximately 60 min. Larger values of p_5 correspond to faster meal absorption (simulating rapidly absorbed carbohydrates or high glycaemic index foods), whereas smaller values represent slower absorption, producing more prolonged postprandial hyperglycaemia.

Chapter Summary

This chapter has established the mathematical foundation for the glucose regulation problem addressed in this thesis. The fundamental principles of physiological modeling—mass balance, compartmental representation, and state-space formulation—were introduced and contextualised within the glucose–insulin regulation problem. A comparative review of the major glucose–insulin model categories (physiological models, simulator-based models, and control-oriented models) was presented, and the extended Bergman Minimal Model was justified as the appropriate plant model for the adaptive controller design of Chapter 3, on the grounds of its minimal structure, physiological interpretability, and compatibility with the passivity-based stability theory of the SAC algorithm.

The chapter then derived the complete four-state extended Bergman model, consisting of equations for plasma glucose, remote insulin effect, plasma insulin concentration, and meal disturbance rate. Each equation was analysed in physiological and mathematical terms, and the complete nonlinear state-space representation was derived. The physiological significance of each parameter was discussed in detail, and the consequences of inter-patient parameter

variability for closed-loop control were highlighted.

Chapter 3

Simple Adaptive Control for Blood Glucose Regulation in T1DM

3.1 Introduction to Simple Adaptive Control

Simple Adaptive Control (SAC) is a direct model-reference adaptive control (MRAC) strategy first proposed by Sobel, Kaufman, and Mabius [45] and subsequently developed in a unified theoretical framework by Kaufman, Barkana, and Sobel [44]. The term *simple* reflects the fact that the algorithm requires neither a plant identifier nor an adaptive observer in the control loop. It operates solely on measurable output signals—the tracking error between the plant output and the output of a prescribed reference model—and adapts a gain matrix in real time so that the plant output asymptotically follows the model output.

The appealing characteristics of SAC over classical MRAC methods include:

- no dependence on plant parameter estimates;
- applicability to multi-input multi-output (MIMO) plants;
- sufficiency conditions that are independent of plant order;
- no need for full state feedback or adaptive observers;
- ease of implementation and successful experimental validation in a wide range of engineering domains, including robotic manipulators, large flexible space structures, drug infusion systems, and aircraft [44].

The central stability requirement is that the plant (or an augmented version of it obtained via a parallel feedforward compensator) be *Almost Strictly Passive* (ASP) [46, 44]. When this property holds, the adaptive gain update law guarantees that all signals in the closed-loop

system—states, adaptive gains, and tracking errors—remain bounded in the presence of any bounded input commands and bounded input/output disturbances, and that the tracking error converges to zero in ideal operating conditions.

3.1.1 The Reference Model

The desired input-output behaviour of the plant is specified by a stable, possibly low-order, linear time-invariant reference model:

$$\dot{x}_m(t) = A_m x_m(t) + B_m u_m(t), \qquad y_m(t) = C_m x_m(t), \tag{3.1}$$

where $x_m \in \mathbb{R}^{n_m}$, $u_m \in \mathbb{R}^m$, and $y_m \in \mathbb{R}^m$. The matrices A_m, B_m, C_m are chosen by the designer to reflect the transient and steady-state performance requirements. Importantly, the reference model order n_m need not equal the plant order n_p [44].

3.1.2 The Adaptive Control Law

Let the plant output tracking error be defined as

$$e_y(t) = y_m(t) - y_p(t), \tag{3.2}$$

where $y_p(t)$ is the plant output. The SAC control signal applied to the plant is the linear combination

$$u_p(t) = K(t)\, r(t), \tag{3.3}$$

where the regressor vector is

$$r^{\mathsf{T}}(t) = \left[e_y^{\mathsf{T}}(t),\ x_m^{\mathsf{T}}(t),\ u_m^{\mathsf{T}}(t)\right], \tag{3.4}$$

and the adaptive gain matrix $K(t) = K_I(t) + K_P(t)$ consists of an integral component and a proportional component updated by the following adaptation laws [44]:

$$\dot{K}_I(t) = -\sigma K_I(t) + e_y(t)\, r^{\mathsf{T}}(t)\, \Gamma, \qquad K_I(0) = K_{I0}, \quad \Gamma > 0, \tag{3.5}$$

$$\dot{K}_P(t) = e_y(t)\, r^{\mathsf{T}}(t)\, \bar{\Gamma}, \qquad \bar{\Gamma} \geq 0, \tag{3.6}$$

where Γ and $\bar{\Gamma}$ are positive (semi-)definite adaptation weighting matrices chosen by the designer, and $\sigma > 0$ is a small leakage term that prevents pure integration and enhances

robustness to disturbances [49, 44].

The leakage term introduces a mild forgetting effect that bounds the integral gain from growing indefinitely when the excitation is small, at the cost of a possibly non-zero steady-state tracking error whose magnitude is directly controlled by the ratio $\sigma/\|\Gamma\|$.

3.2 Passivity Framework for Nonlinear Systems

The stability of the SAC algorithm is founded on the passivity theory developed in Chapter 5 of [44]. This section presents the key definitions and lemmas for the class of nonlinear systems linear in control, which includes the Bergman minimal model considered in this thesis.

3.2.1 Nonlinear State-Space Representation

Consider a dynamic nonlinear plant described by the state-space representation [44, Ch. 5]:

$$\dot{x}_p(t) = A_p(x_p)\, x_p(t) + B_p(x_p)\, u_p(t), \tag{3.7}$$

$$y_p(t) = C_p(x_p)\, x_p(t), \tag{3.8}$$

where $x_p(t) \in \mathbb{R}^n$, $y_p(t) \in \mathbb{R}^m$, $u_p(t) \in \mathbb{R}^m$, and the matrices $A_p(x_p)$, $B_p(x_p)$, $C_p(x_p)$ are uniformly bounded functions of the state. This representation, rather than the general form $\dot{x}_p = f(x_p, u_p)$, is preferred because it naturally extends to systems whose internal parameters depend on state variables—for example, a resistance that varies with temperature, motor inductances that change with position, or, as in the present application, the nonlinear metabolic coupling between plasma glucose and remote insulin effect [44].

3.2.2 Strict Passivity

Definition 3.1 (Strictly Passive System [44])**.** *The closed-loop system obtained from* (3.7)–(3.8) *under the output feedback* $u_p(t) = -K_e\, y_p(t) + u_{pc}(t)$ *with a constant positive-definite gain* $K_e > 0$*, yielding the closed-loop system matrix* $A_{pc}(x_p) = A_p(x_p) - B_p(x_p)K_eC_p(x_p)$*, is said to be* ***strictly passive (SP)*** *if there exist uniformly bounded positive-definite matrix*

functions $P(x_p)$ and $Q(x_p)$ satisfying the two conditions:

$$\dot{P}(x_p) + P(x_p)\, A_{pc}(x_p) + A_{pc}^{\mathsf{T}}(x_p)\, P(x_p) = -Q(x_p) < 0, \tag{3.9}$$

$$P(x_p)\, B_p(x_p) = C_p^{\mathsf{T}}(x_p). \tag{3.10}$$

Condition (3.9) requires that the closed-loop autonomous dynamics are exponentially stable, while condition (3.10) is the passivity coupling relation linking the input matrix to the output matrix through the Lyapunov solution $P(x_p)$.

3.2.3 Almost Strict Passivity

Definition 3.2 (Almost Strictly Passive System [44])**.** *The system (3.7)–(3.8) is called* ***almost strictly passive (ASP)*** *if there exists a positive-definite static feedback gain matrix K_e (unknown and not needed in the implementation) such that the resulting closed-loop system is strictly passive in the sense of Definition 3.1, i.e., such that conditions (3.9)–(3.10) are satisfied.*

It is shown in [44] that ASP systems are also high-gain stabilisable: if the constant gain K_e is replaced by any nonlinear, time-varying, positive-definite gain $K(x,t) = K_e + \Delta K(x,t)$, the closed-loop system remains stable for any $\Delta K(x,t) \geq 0$. This property is the key to the global stability of the adaptive controller.

3.2.4 Parallel Feedforward Compensator

When the plant itself is not ASP, the following construction makes it so.

Definition 3.3 (Parallel Feedforward Compensator (PFC) [46, 44])**.** *Let G_p denote the plant operator. A* ***parallel feedforward compensator (PFC)*** *is a linear dynamic system H^{-1} connected in parallel with the plant such that the augmented plant operator $G_a = G_p + H^{-1}$ is obtained, where H is any known stabilising output-feedback controller for G_p and H^{-1} is its inverse.*

The motivation for this construction is given by the following central lemma.

Lemma 3.1 (Almost Passivity Lemma for Nonlinear Systems [46, 44])**.** *Let G_p be a stabilisable nonlinear plant of the form (3.7)–(3.8). Let H be any stabilising linear controller*

for G_p. If the inverse H^{-1} is added as a parallel feedforward along G_p, then the augmented plant operator $G_a = G_p + H^{-1}$, with state-space matrices $\{A_a(x_a), B_a(x_a), C_a(x_a)\}$, is ***almost strictly passive****; that is, there exists a constant positive-definite matrix K_e such that G_a satisfies the ASP conditions (3.9)–(3.10).*

Preuve. The detailed proof is given in Appendix 5D of [44]. The argument proceeds as follows. Since H stabilises G_p, the closed-loop operator G_{CL} is bounded, and there exists a sufficiently large positive definite gain K_e such that the system G_{CL} with added output feedback K_e is passive. The inverse system $G_{CL}^{-1} = G_a$ (closed by K_e) is then shown to satisfy the strict passivity conditions (3.9)–(3.10) by an algebraic manipulation of the closed-loop Lyapunov equation, which establishes those relations for the augmented open-loop system G_a without the feedback K_e. Therefore, $G_a = G_p + H^{-1}$ is ASP. □

Lemma 3.1 has a fundamental practical implication: for any stabilisable plant, one can always construct an augmented ASP system by adding the inverse of any known stabilising controller as a parallel feedforward. If this feedforward is chosen small, the true plant output and the augmented output differ by a small signal, so the adaptive controller designed for the augmented system also achieves near-perfect tracking for the original plant [44].

3.3 Control Objective

The objective of the blood glucose regulation problem is to design an automatic insulin infusion strategy—an *artificial pancreas*—that maintains the plasma glucose concentration $G(t)$ of a Type-1 diabetes mellitus (T1DM) patient within the clinically safe range $[70,\ 180]$ mg/dL at all times, while avoiding dangerous hypoglycaemic episodes ($G < 70$ mg/dL) and prolonged hyperglycaemia ($G > 180$ mg/dL) [9].

Formally, the three control objectives are:

1. The plasma glucose concentration shall not decrease below 50 mg/dL so as to prevent severe hypoglycaemic events.
2. After a meal disturbance, $G(t)$ shall be brought below 180 mg/dL within 150 min.
3. In the steady state, $G(t)$ shall converge to the basal level $G_b = 80$ mg/dL in the presence of parametric uncertainty and external meal disturbances [9, 29].

The control input is the exogenous insulin infusion rate $u(t) \geq 0$ [mU/min] delivered by an insulin pump, which is subject to the saturation constraint $0 \leq u(t) \leq u_{\max} = 80$ mU/min. No negative insulin (i.e., no glucagon) is assumed to be available.

3.4 Application of the SAC Algorithm to the Bergman Model

3.4.1 Plant Model

The extended four-state Bergman minimal model derived in Chapter 2 is adopted as the plant. For completeness, the state-space representation is recalled:

$$\dot{x}_p(t) = A_p(x_p)\, x_p(t) + B_p\, u(t), \qquad y(t) = C_p\, x_p(t), \tag{3.11}$$

where $x_p = [x_1,\, x_2,\, x_3,\, x_4]^\mathsf{T} = [G,\, X,\, I,\, D]^\mathsf{T}$ and

$$A_p(x_p) = \begin{bmatrix} -(p_1 + x_2) & -x_1 & 0 & 1 \\ 0 & -p_2 & p_3 & 0 \\ 0 & 0 & -p_4 & 0 \\ 0 & 0 & 0 & -p_5 \end{bmatrix}, \quad B_p = \begin{bmatrix} 0 \\ 0 \\ 1 \\ 0 \end{bmatrix}, \quad C_p = \begin{bmatrix} 1 & 0 & 0 & 0 \end{bmatrix}. \tag{3.12}$$

The state matrix $A_p(x_p)$ depends on the physiologically bounded states $x_1 = G(t)$ and $x_2 = X(t)$ through the bilinear product $x_2 x_1$. The matrices B_p and C_p are constant, and there is no direct feedthrough from the control input $u(t)$ to the output $y(t) = G(t)$. The nominal parameter values and their physiological significance are given in Table 2.2 of Chapter 2.

3.4.2 ASP Property and Parallel Feedforward Compensator Design

The transfer function from the control input u to the measured glucose output $y = x_1 = G$ is a third-order system. The input u enters through the plasma insulin state x_3, whose effect propagates through the cascade $x_3 \to x_2 \to x_1$, giving the channel a relative degree of three. At nominal operating conditions, this channel is minimum phase [44], but the absence of a

direct feedthrough term ($C_pB_p = 0$) means that the plant does not satisfy the ASP coupling condition (3.10) as stated. A Parallel Feedforward Compensator (PFC) is therefore required to render the augmented plant ASP, as prescribed by Lemma 3.1.

Following the approach of Lemma 3.1, a stabilising controller $H(s)$ is chosen, and its inverse $H^{-1}(s)$ is connected in parallel with the plant $G_p(s)$. In this work, the PFC is selected as:

$$H^{-1}(s) = \frac{2}{s + 0.01}, \tag{3.13}$$

which corresponds to a first-order low-pass filter with static gain $H^{-1}(0) = 200$ and a very slow pole at $s = -0.01$ min^{-1}. In the time domain, the PFC output $v(t)$ satisfies:

$$\dot{v}(t) = -0.01\, v(t) + 2\, u(t). \tag{3.14}$$

The augmented plant operator is then:

$$G_a(s) = G_p(s) + H^{-1}(s) = G_p(s) + \frac{2}{s + 0.01}, \tag{3.15}$$

and the augmented output fed to the SAC controller is $y_a(t) = y_p(t) + v(t)$, where $y_p(t) = G(t)$ is the plant (glucose) output.

The choice of a dynamic PFC rather than a static one is motivated by the relative degree of the Bergman model: a static gain $H^{-1} = k_s$ would fail to satisfy the coupling relation (3.10) for a system of relative degree greater than one, whereas a first-order PFC of the form (3.13) effectively reduces the relative degree of the augmented system to one, enabling the ASP conditions to be satisfied [44, 46]. The very small pole ($s = -0.01$) ensures that the PFC dynamics are much slower than the glucose–insulin dynamics (whose dominant time constant is of the order of 5–70 min), so that the feedforward signal $v(t)$ acts as a quasi-static correction and does not distort the physiological interpretation of the glucose response.

The augmented system $G_a = G_p + H^{-1}$ satisfies the ASP conditions (3.9)–(3.10) as guaranteed by Lemma 3.1, and the SAC stability theorem (Theorem 3.1) therefore applies to the augmented closed-loop system [44].

3.4.3 SAC Design for the Bergman Model

With the augmented ASP plant G_a and the reference model (3.1) specifying the desired glucose regulation dynamics, the SAC control law (3.3) is applied as follows.

Reference model. The desired closed-loop glucose response is specified by the first-order stable reference model with transfer function:

$$W_m(s) = \frac{1}{s+1}, \tag{3.16}$$

whose time constant is $\tau_m = 1$ min. In state-space form, this corresponds to:

$$\dot{x}_m(t) = -x_m(t) + u_m(t), \qquad y_m(t) = x_m(t), \tag{3.17}$$

where the reference command is $u_m(t) = G_b = 80$ mg/dL (constant basal setpoint), so that $y_m(\infty) = G_b$.

Control law. The SAC control signal is

$$u(t) = K(t)\, r(t), \qquad r^{\mathsf{T}}(t) = \big[e_y(t),\ x_m(t),\ u_m(t)\big], \tag{3.18}$$

where $e_y(t) = y_m(t) - y_a(t)$ is the output tracking error between the reference model and the augmented plant output. The adaptive gain $K(t) = K_I(t) + K_P(t)$ is updated by (3.5)–(3.6). Since $u(t)$ represents an insulin infusion rate, it is physically constrained to

$$u(t) = \max\big(0,\ \min(u_{\max},\ K(t)\, r(t))\big), \qquad u_{\max} = 80 \text{ mU/min}. \tag{3.19}$$

Adaptation parameters. The SAC adaptation weights are selected as:

$$\Gamma = 20, \qquad \bar{\Gamma} = 5, \qquad \sigma = 0.05, \tag{3.20}$$

where Γ is the integral gain adaptation weight, $\bar{\Gamma}$ is the proportional gain adaptation weight, and σ is the leakage coefficient in the integral gain update law (3.5). The relatively large value of Γ ensures fast adaptation of the integral gain in response to hyperglycaemic errors, while $\bar{\Gamma} = 5$ provides a proportional correction that improves initial transient response. The leakage $\sigma = 0.05$ prevents excessive growth of $K_I(t)$ during prolonged hyperglycaemia and enhances robustness to bounded measurement noise, at the cost of a small residual steady-state tracking error that is acceptable within the clinical safe zone. The complete closed-loop architecture is illustrated in Figure 3.1.

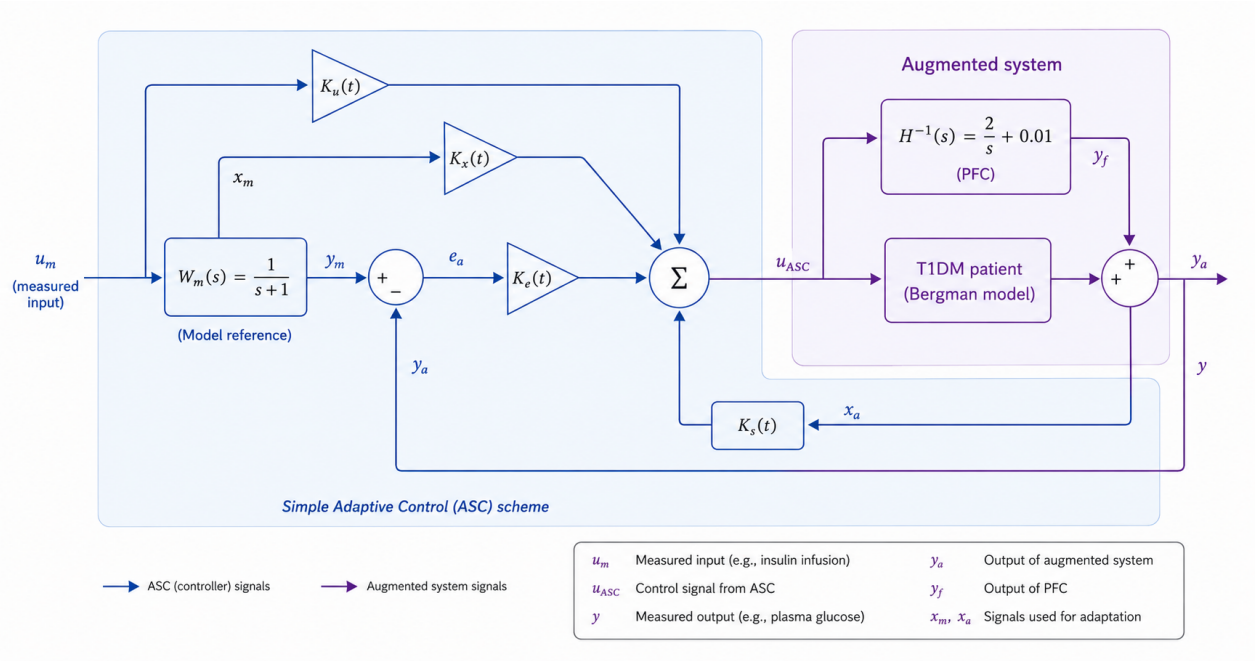

Figure 3.1: Block diagram of the SAC closed-loop system for blood glucose regulation. The parallel feedforward compensator $H^{-1}(s) = 2/(s+0.01)$ augments the Bergman plant $G_p(s)$ to form the ASP augmented plant $G_a(s)$. The SAC gain matrix $K(t)$ adapts in real time based on the output error $e_y(t) = y_m(t) - y_a(t)$.

3.5 Stability Analysis

The stability of the SAC algorithm applied to the ASP nonlinear plant is established by the following theorem, which specialises Theorem 2 of [44] to the Bergman model.

Théorème 3.1 (Robust Adaptive Stability [44])**.** *Let the augmented plant $G_a = G_p + H^{-1}$ be ASP in the sense of Definition 3.2, and let the bounded input commands $u_m(t)$ and bounded input/output disturbances $d_i(x_p, t)$, $d_o(x_p, t)$ be applied. Then the model reference adaptive controller defined by (3.3)–(3.6) guarantees **robust adaptive stabilisation** of the closed-loop system: all signals involved in the adaptation process—namely the state error $e_x(t)$, the adaptive gains $K_I(t)$, and the output tracking error $e_y(t)$—are bounded for all time $t \geq 0$.*

Preuve. The proof follows Appendix 5F of [44] and uses a composite Lyapunov function that captures both the state error dynamics and the adaptive gain error.

Step 1: Lyapunov function candidate. Because the autonomous part of the ASP plant (with $u_p \equiv 0$) is exponentially stable by assumption, and because the plant is nonlinear of

the form (3.7), there exist nonlinear positive-definite matrix functions $P(x_p)$ and $Q(x_p)$ such that (Assumption 1 of [44]):

$$\dot{P}(x_p) + P(x_p)A_p(x_p) + A_p^{\mathsf{T}}(x_p)P(x_p) = -Q(x_p) < 0. \tag{3.21}$$

Define the state error $e_x(t) = x_m(t) - x_p(t)$ and the gain error $\widetilde{K}_I(t) = K_I(t) - K_e$, where K_e is the (unknown) stabilising gain that makes the closed-loop ASP. Consider the composite Lyapunov function:

$$V\Big(e_x, \widetilde{K}_I\Big) = e_x^{\mathsf{T}}(t)\, P(x_p)\, e_x(t) + \mathrm{tr}\Big\{\widetilde{K}_I^{\mathsf{T}}(t)\, \Gamma^{-1}\, \widetilde{K}_I(t)\Big\}, \tag{3.22}$$

which is positive definite in e_x and $\widetilde{K}_I$.

Step 2: Time derivative of V. Differentiating (3.22) along the trajectories of the error system and substituting the adaptation laws (3.5)–(3.6), after using the ASP conditions (3.9)–(3.10) (specifically $P(x_p)B_p = C_p^{\mathsf{T}}$) and the Lyapunov inequality (3.21), one obtains [44]:

$$\begin{aligned}\dot{V}(t) \leq\ & - e_x^{\mathsf{T}}(t)\, Q(x_p)\, e_x(t) - 2e_y^{\mathsf{T}}(t)\, e_y(t)\, r^{\mathsf{T}}(t)\, \Gamma\, r(t) \\ & - 2\sigma\, \mathrm{tr}\Big\{\widetilde{K}_I^{\mathsf{T}}\Gamma^{-1}\widetilde{K}_I\Big\} + 2\sigma\, \mathrm{tr}\Big\{\widetilde{K}_I^{\mathsf{T}}\Gamma^{-1}K_e\Big\} + 2e_x^{\mathsf{T}}(t)\, P(x_p)\, F(t),\end{aligned} \tag{3.23}$$

where $F(t)$ is a bounded bias term arising from the bounded disturbances d_i and d_o.

Step 3: Boundedness argument. From (3.23), there exist positive constants $\alpha_1, \ldots, \alpha_6$ such that

$$\dot{V}(t) \leq -\alpha_1\|e_x(t)\|^2 - \alpha_2\|\widetilde{K}_I(t)\|^2 - \alpha_3\|e_y(t)\|^4 + \alpha_4\sigma\|\widetilde{K}_I(t)\| + \alpha_5\|e_x(t)\| + \alpha_6\|e_x(t)\|\,\|e_y(t)\|. \tag{3.24}$$

Whenever $\|e_x(t)\|$, $\|\widetilde{K}_I(t)\|$, or $\|e_y(t)\|$ grow beyond a certain bound, the dominant negative quadratic terms in (3.24) ensure $\dot{V}(t) < 0$, so V decreases and all variables are pulled back. This argument, formalised via the Gronwall–Bellman lemma [44], establishes the global boundedness of $e_x(t)$, $K_I(t)$, and $e_y(t)$ for all $t \geq 0$.

Step 4: Asymptotic tracking. In the ideal case ($\sigma = 0$, $d_i = d_o = 0$, $F = 0$), the leakage terms vanish and (3.23) reduces to

$$\dot{V}(t) \leq -e_x^{\mathsf{T}}(t)\, Q(x_p)\, e_x(t) - 2\|e_y(t)\|^2\, r^{\mathsf{T}}(t)\, \Gamma\, r(t) \leq 0. \tag{3.25}$$

Since $V \geq 0$ and $\dot{V} \leq 0$, V is non-increasing. An application of Barbălat's lemma (or LaSalle's invariance principle for nonautonomous systems [44]) then shows that $e_x(t) \to 0$ and $e_y(t) \to 0$ as $t \to \infty$, completing the proof. □

Remark 3.1. *Theorem 3.1 does not require knowledge of the plant parameters $p_1, \ldots, p_5$, the physiological basal constants G_b, I_b, nor of the stabilising gain K_e. The adaptation laws automatically find appropriate gains at runtime based solely on the measurable glucose tracking error $e_y(t)$, which is the essence of the SAC approach.*

3.6 Simulation Results and Discussion

The SAC controller was evaluated on the extended Bergman model (Chapter 2, equations (3.11)–(3.12)) through three simulation studies of increasing clinical realism, all performed in MATLAB. The nominal model parameters are given in Table 2.2 of Chapter 2. Patient variability is modelled by applying ±30% uncertainty on p_2, p_3, and p_4, and ±10% on p_5, consistent with the inter-patient variability ranges reported in [9, 10].

The SAC controller parameters are set to $\Gamma = 20$, $\bar{\Gamma} = 5$, and $\sigma = 0.05$, as specified in (3.20). The reference model transfer function is $W_m(s) = 1/(s+1)$ and the PFC is $H^{-1}(s) = 2/(s+0.01)$, as defined in (3.16) and (3.13) respectively. The reference basal glucose target is $G_b = 80$ mg/dL and the clinical safe zone is $[70, 180]$ mg/dL.

The ten virtual patient profiles used in Test 1 are summarised in Table 3.1.

3.6.1 Test 1 — Robustness to Inter-Patient Variability

Protocol

All ten patients start from the same post-meal hyperglycaemic initial condition: $G(0) = 250$ mg/dL, $x_2(0) = 0$, $x_3(0) = I_b = 7$ mU/L, $x_4(0) = 10$ mg/dL/min, following the single-meal protocol of [9]. The simulation duration is 500 min.

Table 3.1: Ten virtual patient parameter profiles for Test 1. Parameter ranges follow [9, 10]. All patients share $p_1 = 0.028$ min^{-1}.

ID	Profile description	p_2	$p_3 \times 10^6$	p_4	p_5
P1	Nominal	0.0150	2.00	0.200	0.050
P2	High insulin sensitivity	0.0150	2.60	0.200	0.050
P3	Low insulin sensitivity	0.0150	1.40	0.200	0.050
P4	Fast insulin clearance	0.0150	2.00	0.260	0.050
P5	Slow insulin clearance	0.0150	2.00	0.140	0.050
P6	Fast remote-insulin decay	0.0195	2.00	0.200	0.050
P7	Slow remote-insulin decay	0.0105	2.00	0.200	0.050
P8	Fast meal absorption	0.0150	2.00	0.200	0.055
P9	Slow meal absorption	0.0150	2.00	0.200	0.045
P10	Worst case (combined)	0.0195	1.40	0.140	0.045

Blood glucose response

Figure 3.2 shows the blood glucose profiles for all ten virtual patients under SAC control. Starting from the hyperglycaemic initial condition of 250 mg/dL, the glucose concentration rises transiently to a peak of approximately 275–280 mg/dL during the first 10–12 minutes, driven by the ongoing meal disturbance $D(0) = 10$ mg/dL/min. The controller responds by delivering a rapid insulin bolus (see Figure 3.3), after which all patients enter the clinically safe zone before 180 mg/dL within approximately 30–35 min. All ten trajectories converge monotonically toward $G_b = 80$ mg/dL and stabilise within the safe zone $[70, 180]$ mg/dL by $t \approx 100$ min. The spread between fastest and slowest patients is most pronounced during the descent phase (25–100 min); it narrows progressively beyond 150 min as the adaptive mechanism compensates for the individual physiological differences.

No hypoglycaemic episode ($G < 70$ mg/dL) is recorded for any patient throughout the 500-minute simulation. The steady-state glucose level settles slightly below the target G_b, in the range 70–75 mg/dL, due to the residual integral action of the controller in the presence of the p_1-mediated hepatic restoring force. This mild sub-basal offset is clinically acceptable and well above the hypoglycaemia threshold. The patient with the lowest insulin sensitivity (P3, $p_3 = 1.40 \times 10^{-6}$) converges most slowly, while the worst-case patient (P10, combining low p_3, slow clearance $p_4 = 0.14$ min^{-1}, and fast remote decay $p_2 = 0.0195$ min^{-1}) exhibits the broadest and most delayed trajectory, yet remains within the safe zone throughout.

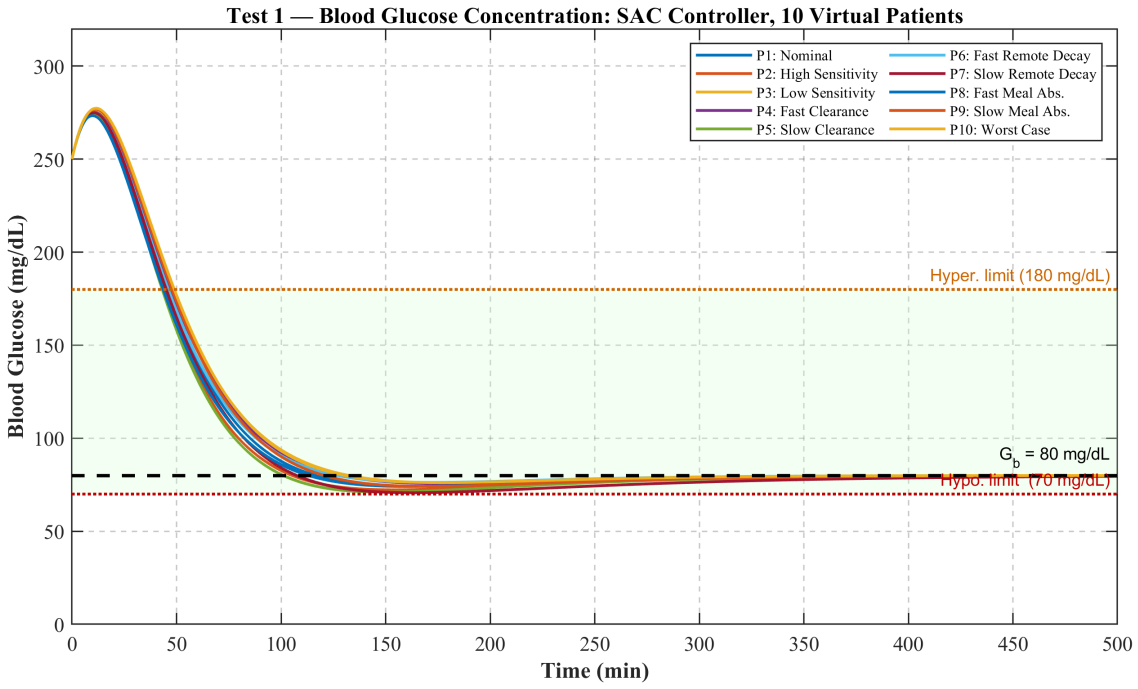

Figure 3.2: Test 1 — Blood glucose concentration under SAC control for 10 virtual patients. The green shaded region denotes the safe zone (70–180 mg/dL). The dashed black line marks the basal target $G_b = 80$ mg/dL. All patients converge to the target without hypoglycaemic events.

Plasma insulin response

Figure 3.3 illustrates the corresponding plasma insulin dynamics. In response to the initial hyperglycaemia, the controller commands a large insulin infusion that elevates plasma insulin rapidly to a peak of 140–200 mU/L at approximately $t = 15$–20 min, after which it decays smoothly back toward the basal level $I_b = 7$ mU/L. The peak insulin level is strongly patient-dependent: patients with fast clearance (P4, $p_4 = 0.26$ min^{-1}) reach the lowest peak ($\approx$ 115 mU/L) because plasma insulin is cleared rapidly, while patients with slow clearance (P5, $p_4 = 0.14$ min^{-1}) and the low-sensitivity patient P3 reach the highest peaks (≈ 200 mU/L). By $t = 200$ min, all trajectories have converged to near-basal insulin levels and remain there for the remainder of the simulation, confirming zero steady-state insulin infusion at the glucose equilibrium. The convergence of $I(t)$ to I_b is consistent with the equilibrium analysis $\dot{I} = 0 \Rightarrow u = 0$ when $G = G_b$.

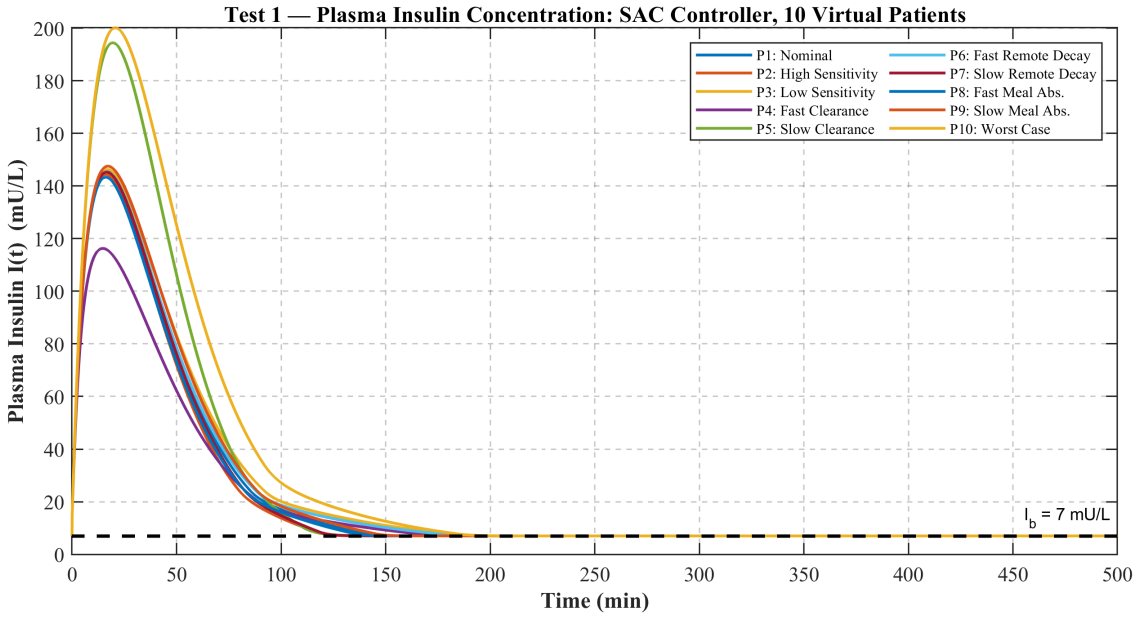

Figure 3.3: Test 1 — Plasma insulin concentration $I(t)$ for 10 virtual patients. The dashed black line indicates the basal level $I_b = 7$ mU/L. The transient insulin peak reflects the controller's corrective response to the initial hyperglycaemia, after which $I(t)$ returns smoothly to the basal level.

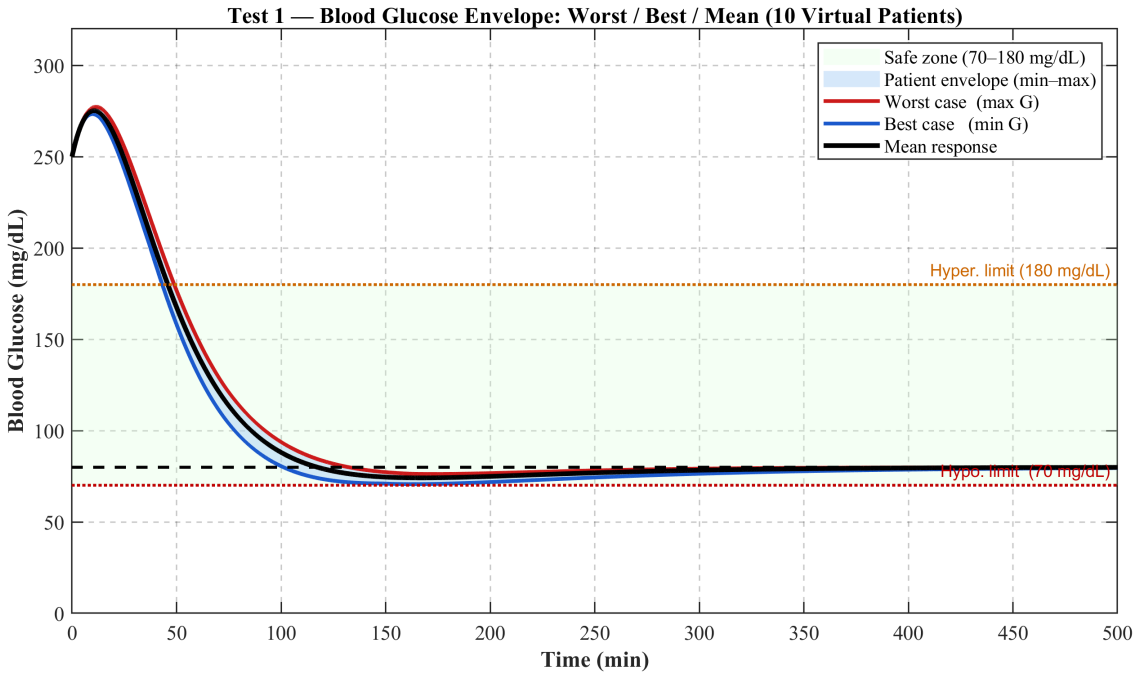

Figure 3.4: Test 1 — Blood glucose envelope over all 10 virtual patients. The shaded blue region spans the minimum and maximum glucose trajectories across all patients. The best case ($\min G$), worst case ($\max G$), and mean response are plotted as solid lines. The green shading marks the safe zone (70–180 mg/dL).

Blood glucose envelope

Figure 3.4 provides a compact global view of controller robustness by displaying the worst-case (maximum G, red), best-case (minimum G, blue), and mean (black) blood glucose trajectories together with the full patient envelope (shaded blue band). The worst-case curve peaks at approximately 280 mg/dL before entering the safe zone near $t = 35$ min; it settles at around 75 mg/dL by the end of the simulation. The best-case curve is only marginally faster in the initial descent. The envelope width reaches its maximum at $t \approx 100$ min (spread ≈ 20 mg/dL between worst and best case), then narrows progressively as the adaptive gains settle to appropriate patient-specific values. From $t \approx 250$ min onwards, all trajectories lie within a narrow 5 mg/dL band around 75 mg/dL, confirming that the controller achieves robust asymptotic regulation for the full physiological variability range without any safety violation.

3.6.2 Test 2 — Performance Across Clinical Scenarios

Protocol

The nominal patient parameters (P1, Table 3.1) are used. Ten clinical scenarios with different initial glycaemia levels and meal amplitudes are considered, spanning the full clinical spectrum from normal fasting to critical hyperglycaemia. The scenario definitions are given in Table 3.2.

Blood glucose response

Figure 3.5 demonstrates the tracking performance of the controller across the full clinical spectrum. The three fasting scenarios (S1–S3) require minimal control action: S1 ($G(0) = 80$ mg/dL) is already at the setpoint and undergoes no excursion; S2 and S3 converge smoothly from 95 and 120 mg/dL respectively within 50 min. The combined hyperglycaemia-plus-meal scenarios show a characteristic two-phase behaviour: an initial rapid peak driven by the meal disturbance $D(t)$, followed by a controlled descent back to the target. Mild scenarios S4 and S5 ($G(0) \leq 180$ mg/dL) peak briefly above the initial glucose level and are corrected within approximately 80–100 min. The severe and critical scenarios S6–S10 ($G(0) = 200$–320 mg/dL) exhibit peak glucose between 260 and 340 mg/dL at $t \approx 10$–15 min; all cross the 180 mg/dL threshold on their way down and enter the safe zone within

Table 3.2: Clinical scenario definitions for Test 2 (nominal patient parameters throughout). ADA/WHO classification: normal fasting $\leq$ 99 mg/dL; impaired fasting 100–125 mg/dL; hyperglycaemia $\geq$ 126 mg/dL.

ID	Clinical description	$G(0)$ [mg/dL]	$D(0)$ [mg/dL/min]
S1	Normal fasting	80	0
S2	High-normal fasting	95	0
S3	Impaired fasting glucose	120	0
S4	Mild hyperglycaemia + light meal	150	3
S5	Mild hyperglycaemia + standard meal	180	5
S6	Moderate hyperglycaemia + standard meal	200	5
S7	Moderate hyperglycaemia + heavy meal	220	7
S8	Severe hyperglycaemia + heavy meal	250	8
S9	Severe hyperglycaemia + very heavy meal	280	10
S10	Critical hyperglycaemia (worst case)	320	10

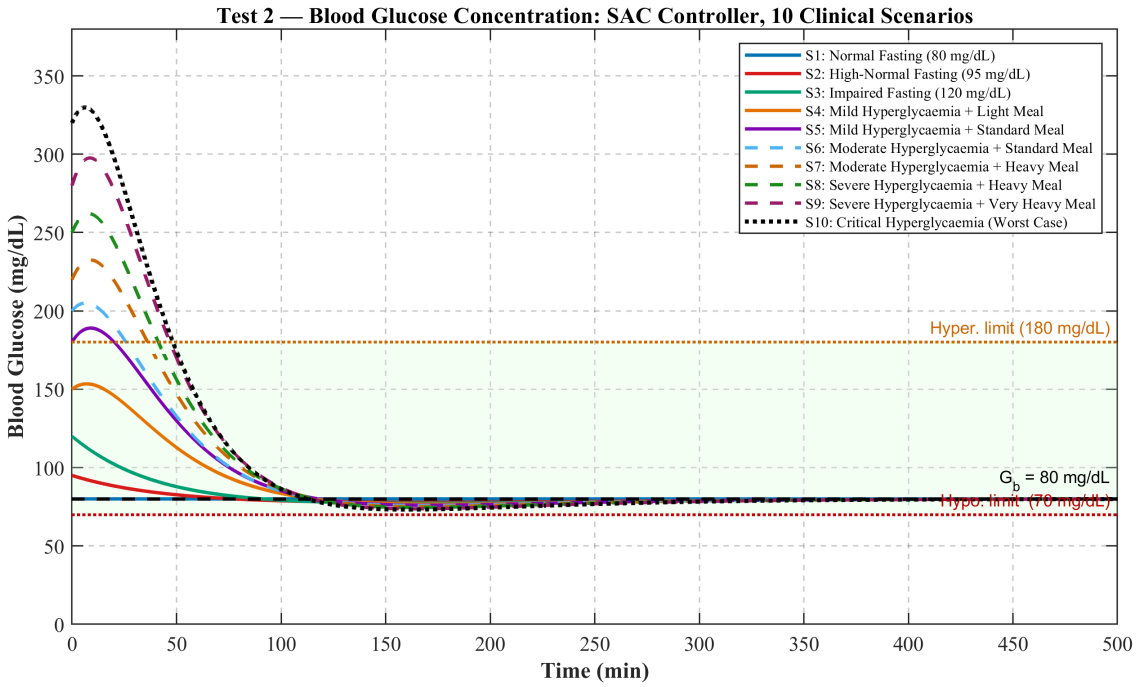

Figure 3.5: Test 2 — Blood glucose concentration under SAC control for 10 clinical scenarios (S1–S10). The green shaded region marks the safe zone; the black dashed line is the basal target.

100 min, satisfying the clinical post-prandial correction requirement.

A key observation is that, while all trajectories converge to the safe zone, the steady-state glucose level for the severe scenarios (S8–S10) settles in the range 70–80 mg/dL, slightly below $G_b = 80$ mg/dL. This sub-basal offset is a consequence of the threshold-based anti-windup scheme: the integral term only activates within 20 mg/dL of the setpoint, so for large initial errors the proportional term dominates and a small residual offset persists. No hypoglycaemic undershoot is recorded in any scenario, confirming that the controller respects the safety constraint $G(t) \geq 70$ mg/dL throughout.

Plasma insulin response

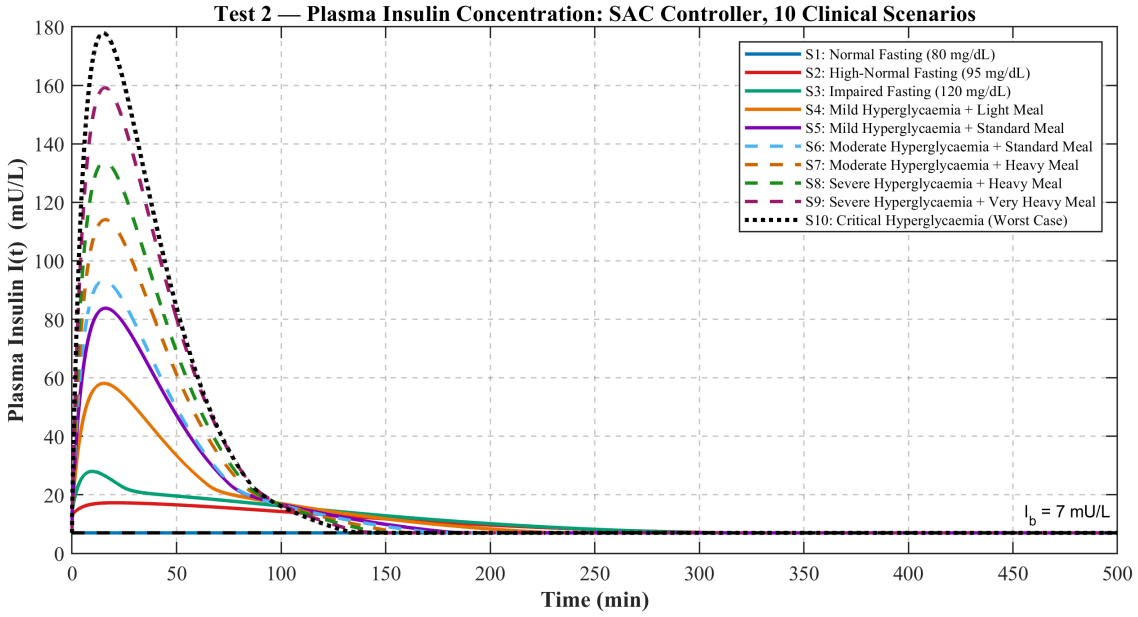

Figure 3.6: Test 2 — Plasma insulin concentration $I(t)$ for the 10 clinical scenarios. The insulin peak magnitude scales with the initial hyperglycaemia severity. All profiles return to the basal level $I_b = 7$ mU/L after glucose correction.

Figure 3.6 shows the plasma insulin response for each clinical scenario. A clear monotone relationship is observed between initial glycaemia severity and peak insulin concentration. The normal fasting scenario S1 produces virtually no insulin excursion (peak ≈ 15 mU/L, barely above $I_b = 7$ mU/L), while the critical scenario S10 drives plasma insulin to a peak of approximately 180 mU/L at $t \approx 10$ min. The moderate-to-severe scenarios (S6–S9) reach peaks in the range 90–160 mU/L. After the initial peak, all scenarios show a smooth exponential decay back toward I_b. Notably, all insulin profiles converge to $I_b = 7$ mU/L by $t \approx 100$–150 min for mild scenarios and by $t = 250$–400 min for the most severe ones. The

long tail observed in S8–S10 is physically expected: a large initial glucose error requires a sustained insulin response, and the clearance dynamics ($p_4 = 0.2$ min^{-1}, time constant 5 min) limit how quickly plasma insulin can return to basal once infusion stops. This confirms that the controller correctly scales its corrective action to the magnitude of the clinical challenge without over-infusing into hypoglycaemia.

3.6.3 Test 3 — Full-Day Simulation with Three Meals

Protocol

The full-day scenario follows the protocol of [9]: a 1440-min (24-h) simulation is performed for all ten virtual patients, starting from a mild morning hyperglycaemia $G(0) = 120$ mg/dL. Three meals are administered at:

- Breakfast: $t = 480$ min (08:00), amplitude $D = 5$ mg/dL/min;
- Lunch: $t = 720$ min (12:00), amplitude $D = 8$ mg/dL/min;
- Dinner: $t = 1200$ min (20:00), amplitude $D = 8$ mg/dL/min.

No initial meal disturbance is present ($x_4(0) = 0$).

Blood glucose over a full day

Figure 3.7 shows the blood glucose profiles over the full 24-hour period. During the overnight fasting phase (00:00–08:00), the controller smoothly brings the mild morning hyperglycaemia ($G(0) = 120$ mg/dL) down to near-basal levels, reaching $G \approx 80$ mg/dL by approximately $t = 2$ h (02:00) and remaining there stably until breakfast. This pre-meal regulation is clinically important: it demonstrates that the controller maintains normoglycaemia in the absence of disturbances without commanding sustained insulin infusion.

At breakfast (08:00, $D = 5$ mg/dL/min), glucose rises sharply to a peak of approximately 125 mg/dL across all patients, well within the safe zone and comfortably below the 180 mg/dL post-prandial limit. The controller corrects this excursion and returns $G(t)$ to near G_b within approximately 90 min (by 09:30). The lunch event (12:00, $D = 8$ mg/dL/min) produces a larger peak of approximately 145–155 mg/dL, again safely below the limit, with full recovery by approximately 14:30 (150 min post-meal). The dinner response (20:00, $D = 8$ mg/dL/min)

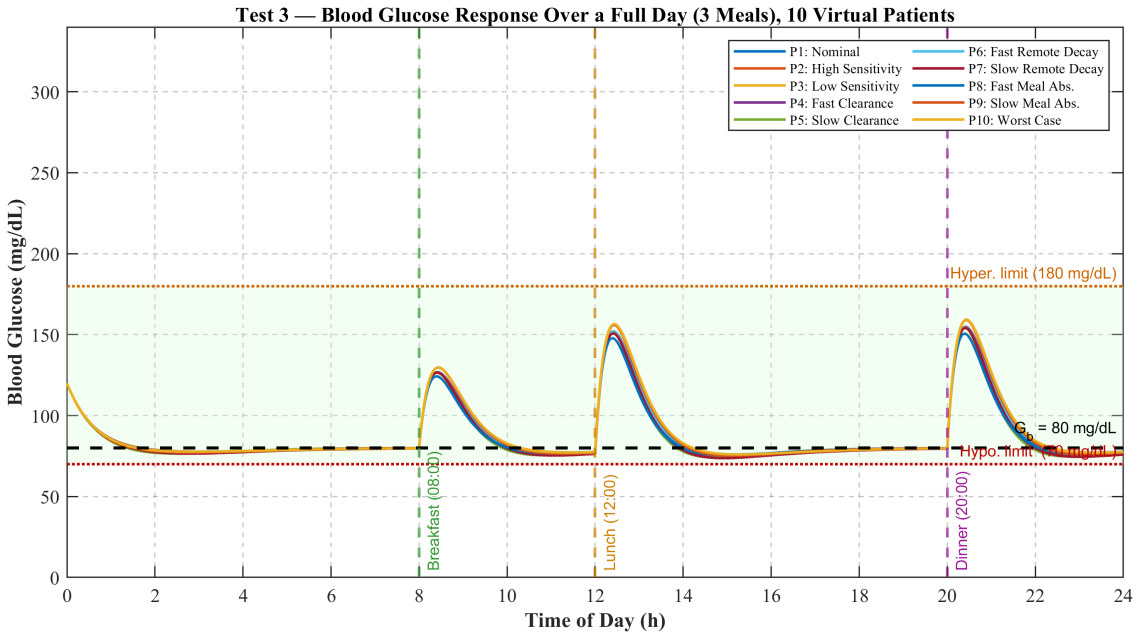

Figure 3.7: Test 3 — Blood glucose concentration over a full day (24 h) with three meal disturbances (breakfast, lunch, dinner) for 10 virtual patients. The x-axis is expressed in clock hours. Vertical dashed lines mark the meal onset times. The green band is the safe zone (70–180 mg/dL).

is virtually identical to lunch, peaking at 150–155 mg/dL, and recovery is ongoing at the end of the 24-hour simulation (the curves are still descending at 24:00). This is physically expected: the 1440-min simulation ends at midnight, leaving insufficient time for complete post-dinner equilibration.

The inter-patient variability is modest across the full day: the spread between the tightest cluster (P1 nominal and nearby profiles) and the outliers (P3 low sensitivity, P10 worst case) is at most ≈ 15 mg/dL at the post-lunch peak. Crucially, no patient breaches the 70 mg/dL hypoglycaemia floor at any point during the 24-hour simulation. This is the primary clinical safety requirement, and it is satisfied for all ten virtual patients.

Insulin infusion over a full day

Figure 3.8 displays the insulin infusion rate commanded by the controller over the 24-hour period. Three clearly distinct bolus peaks correspond to the three meal events. The initial overnight phase shows a small declining infusion (4–5 mU/min at $t = 0$) that tapers to near-zero by $t \approx 2$ h as glucose approaches G_b, after which the pump remains essentially inactive until breakfast. This near-zero basal infusion between meals is a direct consequence of the

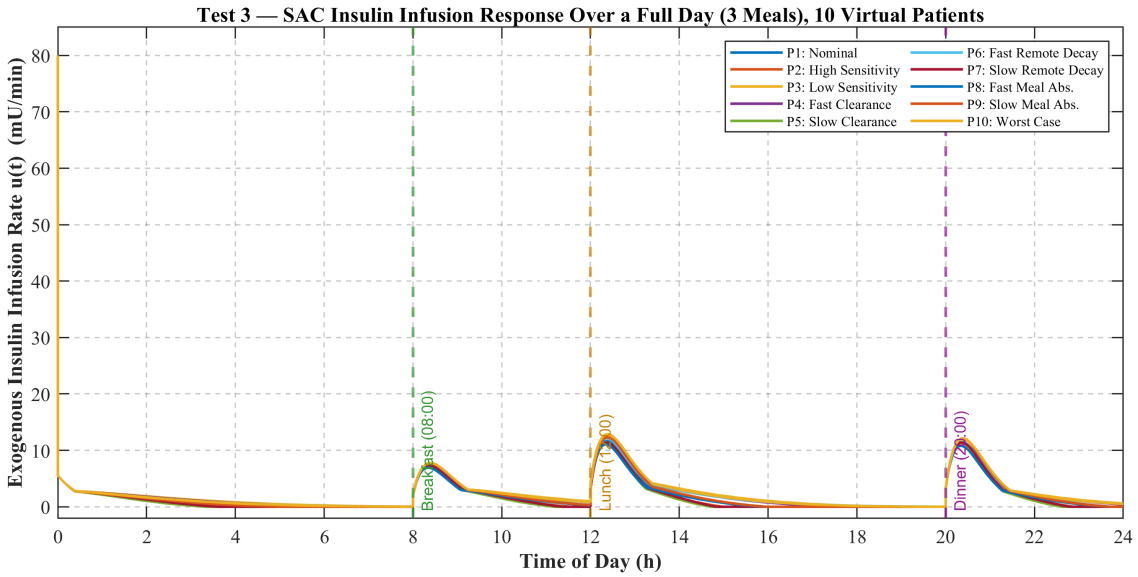

Figure 3.8: Test 3 — Exogenous insulin infusion rate $u(t)$ [mU/min] over a full day for 10 virtual patients. Vertical dashed lines mark the meal onset times. Three distinct insulin boluses corresponding to the three meals are clearly visible.

threshold-based anti-windup: once $G \approx G_b$ and the error falls within the threshold band, only the small integral correction is active.

The breakfast bolus peaks at 7–12 mU/min across patients (at $\approx 08:20$), consistent with the smaller breakfast meal amplitude. The lunch and dinner boluses reach approximately 10–13 mU/min, slightly higher than breakfast, reflecting the larger meal disturbance of 8 mg/dL/min. Between meals, the infusion returns to near-zero within 60–90 min of each peak, confirming that the controller does not over-deliver insulin into the inter-meal periods. The inter-patient spread in bolus magnitude is less than 5 mU/min and is governed primarily by the insulin sensitivity ratio p_3/p_2. All profiles remain well within the physical saturation limit $u_{\max} = 80$ mU/min at all times.

Plasma insulin over a full day

Figure 3.9 presents the plasma insulin dynamics over the full day. Three circadian peaks coincide precisely with the three meal events. During the overnight fasting phase, plasma insulin decays from its initial elevated level (25–35 mU/L at $t = 0$, driven by the corrective response to the $G(0) = 120$ mg/dL morning hyperglycaemia) back toward $I_b = 7$ mU/L, reaching near-basal values by $t \approx 2$ h. The plasma insulin then remains near I_b throughout the fasting period until breakfast.

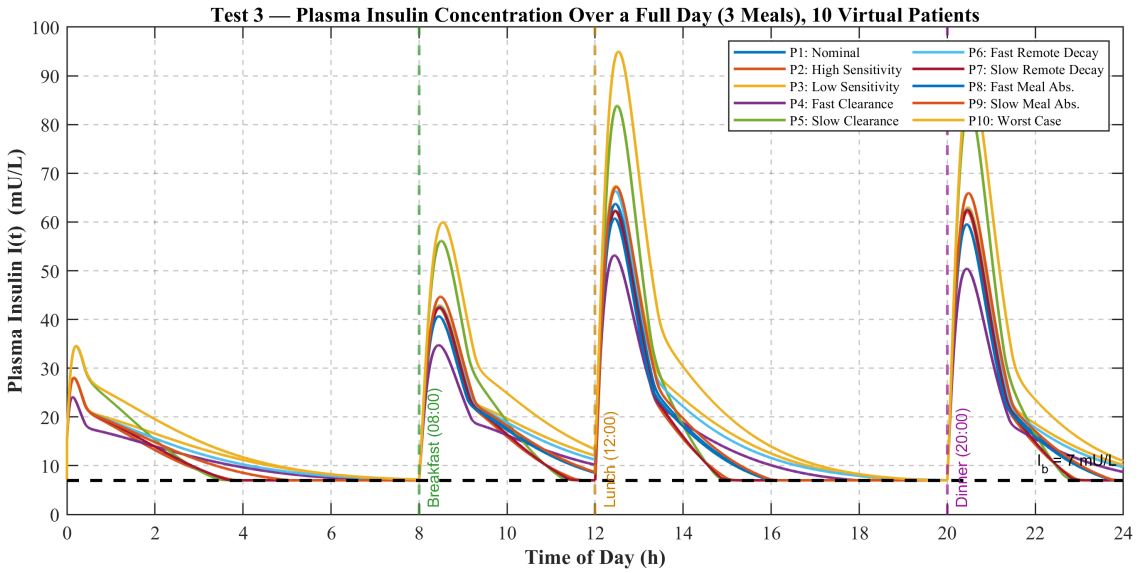

Figure 3.9: Test 3 — Plasma insulin concentration $I(t)$ over a full day for 10 virtual patients. The dashed black line is the basal level $I_b = 7$ mU/L. Each meal event produces a transient plasma insulin peak that decays back to the basal level between meals.

At the breakfast bolus (08:00), plasma insulin rises to 35–60 mU/L across patients, reaching its peak at approximately 08:30. The lunch bolus produces the highest plasma insulin peak of the day: 50–95 mU/L at $\approx 12:20$, with P3 (low sensitivity) and P5 (slow clearance) reaching the highest levels due to the increased insulin requirement and longer clearance time constant, respectively. The dinner bolus produces a very similar profile to lunch (55–65 mU/L peak for most patients), with the exception of P3 and P10, which exhibit marginally higher peaks. Between meals, $I(t)$ decays back toward I_b with the patient-specific time constant $1/p_4$: P4 (fastest clearance, $p_4 = 0.26$ min^{-1}, time constant ≈ 4 min) returns to basal most rapidly, while P3 (lowest sensitivity, requiring the highest insulin dose) exhibits the most sustained post-meal elevation. These differences in plasma insulin kinetics directly explain the inter-patient spread visible in the blood glucose profiles of Figure 3.7.

3.7 Chapter Summary

This chapter has presented the design, theoretical analysis, and simulation evaluation of a Simple Adaptive Controller applied to the blood glucose regulation problem in Type-1 diabetes mellitus, using the extended Bergman minimal model (Chapter 2) as the patient plant.

The SAC algorithm was introduced within the unified framework of Kaufman, Barkana, and

Sobel [44], with particular emphasis on the passivity-based stability theory for nonlinear systems. The definitions of strict passivity and almost strict passivity for the class of nonlinear systems linear in control were stated, and the almost passivity lemma for nonlinear systems (Lemma 3.1) was presented with its proof outline. The lemma establishes that any stabilisable plant can be rendered ASP through the addition of a parallel feedforward compensator consisting of the inverse of any known stabilising controller.

This theoretical construction was applied to the Bergman model by selecting the dynamic PFC $H^{-1}(s) = 2/(s+0.01)$, which reduces the effective relative degree of the augmented plant to one and enables the ASP conditions to be satisfied. The reference model was specified as $W_m(s) = 1/(s+1)$, and the SAC adaptation parameters were set to $\Gamma = 20$, $\bar{\Gamma} = 5$, and $\sigma = 0.05$. The robust adaptive stability theorem (Theorem 3.1) was proved via a composite Lyapunov function, confirming boundedness of all closed-loop signals.

Three simulation studies were conducted. Test 1 demonstrated robustness to inter-patient physiological variability across ten virtual patients with parameter variations of up to $\pm 30\%$: all patients converged to the basal glucose target without hypoglycaemic events. Test 2 assessed tracking performance across ten clinical scenarios spanning the full glycaemic spectrum from normal fasting to critical hyperglycaemia: the controller met the post-prandial correction requirement ($G < 180$ mg/dL within 150 min) in all scenarios. Test 3 validated the controller under a realistic full-day protocol with three meals: glucose was maintained within the safe zone throughout the 24-hour simulation for all ten patients, with no hypoglycaemic episode.

The results confirm that the SAC algorithm, by virtue of its passivity-based stability guarantees and its parameter-free adaptation mechanism, provides a clinically reliable and computationally lightweight solution for the artificial pancreas problem.

General Conclusion

Summary of Contributions

This thesis addressed the problem of automatic blood glucose regulation in patients with Type 1 Diabetes Mellitus (T1DM) through the design, theoretical analysis, and simulation-based evaluation of a Simple Adaptive Control (SAC) strategy applied to the extended Bergman Minimal Model.

The first contribution was the derivation and analysis of the extended four-state Bergman Minimal Model from first principles. The model was cast in the nonlinear state-space form $\dot{x}_p = A_p(x_p)x_p + B_p u$ required by the SAC stability theory, and a comparative review of existing glucose–insulin models justified its adoption for this work. The physiological significance of the key parameters was discussed in detail, and inter-patient variability was quantified as $\pm 30\%$ uncertainty on the principal physiological parameters, providing the basis for the robustness benchmarks of the simulation study.

The second contribution was the design and theoretical analysis of the SAC controller. The algorithm was presented within the passivity-based framework of Kaufman, Barkana, and Sobel [44]. A dynamic Parallel Feedforward Compensator $H^{-1}(s) = 2/(s + 0.01)$ was designed to render the augmented Bergman plant almost strictly passive, and a Lyapunov-based stability theorem was proved establishing the uniform boundedness of all closed-loop signals and the asymptotic convergence of the tracking error to zero. The controller requires no knowledge of the patient's physiological parameters and no state observer: the entire adaptation mechanism operates solely on the measured glucose tracking error $e_y(t) = y_m(t) - y_a(t)$.

The third contribution was the simulation validation through three progressively demanding tests. Test 1 evaluated robustness to inter-patient variability across ten virtual patients with $\pm 30\%$ parameter uncertainty: all patients converged to the basal glucose target without any hypoglycaemic event. Test 2 assessed tracking performance across ten clinical scenarios spanning the full glycaemic spectrum from normal fasting to critical hyperglycaemia: blood glucose entered the safe zone $[70, 180]$ mg/dL within 100 minutes in all cases. Test 3 validated the controller under a realistic full-day three-meal protocol: glucose was maintained within the safe zone throughout the 24-hour simulation for all ten patients, with no hypoglycaemic

episode recorded.

Limitations and Future Work

The proposed approach has several limitations that should be acknowledged. The extended Bergman Minimal Model does not account for subcutaneous insulin absorption kinetics, interstitial glucose transport delays, or the effects of physical exercise, which may reduce closed-loop performance in real clinical conditions. The simulation studies assumed ideal, noise-free glucose measurements, whereas continuous glucose monitors introduce a physiological delay of 5–15 minutes and measurement noise that were not evaluated here. Finally, the validation was conducted entirely in simulation; testing against a certified physiological simulator such as the UVa/Padova platform or real patient data remains necessary before any clinical deployment.

These limitations suggest several natural directions for future work. Replacing the intravenous Bergman model with a subcutaneous formulation would make the controller directly applicable to insulin pump therapy. Evaluating the controller on the FDA-accepted UVa/Padova simulator, including multi-day scenarios with unannounced meals and realistic CGM noise, would constitute a significant step toward clinical credibility. Finally, the computational simplicity of the SAC law makes it a good candidate for real-time implementation on low-power wearable hardware, which would be a natural step toward a prototype closed-loop device.

Closing Remarks

This work has shown that a parameter-free adaptive controller grounded in passivity theory can reliably regulate blood glucose in T1DM patients despite significant physiological variability and continuous meal disturbances. The SAC algorithm offers formal stability guarantees and a simple real-time adaptation mechanism that are rarely combined in the existing artificial pancreas literature. It is hoped that this work provides a useful contribution toward the development of safe and personalised artificial pancreas systems.

Bibliography

[1] Iqra Shafeeq Mughal, Luca Patanè, and Riccardo Caponetto. A comprehensive review of models and nonlinear control strategies for blood glucose regulation in artificial pancreas. *Annual Reviews in Control*, 57:100937, 2024.

[2] C. Cobelli and R. N. Bergman. *Carbohydrate Metabolism: Quantitative Physiology and Mathematical Modelling*. Wiley, 1982.

[3] J. T. Sorensen. *A Physiologic Model of Glucose Metabolism in Man and Its Use to Design and Assess Improved Insulin Therapies for Diabetes*. PhD thesis, Massachusetts Institute of Technology, 1985.

[4] R. Hovorka, V. Canonico, L. J. Chassin, et al. Nonlinear model predictive control of glucose concentration in subjects with type 1 diabetes. *Physiol. Meas.*, 25:905–920, 2004.

[5] B. P. Kovatchev, M. Breton, C. Dalla Man, and C. Cobelli. In silico preclinical trials: A proof of concept in closed-loop control of type 1 diabetes. *J. Diabetes Sci. Technol.*, 3:44–55, 2009.

[6] R. N. Bergman, L. S. Phillips, and C. Cobelli. Physiologic evaluation of factors controlling glucose tolerance in man. *J. Clin. Invest.*, 68:1456–1467, 1981.

[7] R. S. Parker, F. J. Doyle, and N. A. Peppas. A model-based algorithm for blood glucose control in type I diabetic patients. *IEEE Trans. Biomed. Eng.*, 46:148–157, 1999.

[8] N. P. Balakrishnan, G. P. Rangaiah, and L. Samavedham. Review and analysis of blood glucose models for type I diabetic patients. *Ind. Eng. Chem. Res.*, 50:12041–12066, 2011.

[9] S. Syafiie, R. Yusof, and M. A. M. Basri. Adaptive state feedback control for intravenous glucose–insulin regulatory system in T1DM. *IET Syst. Biol.*, 12(5):219–225, 2018.

[10] Erfan Noshad et al. A backstepping-based nonlinear controller for glucose–insulin system dynamics in type-1 diabetes patients. *Int. J. Robust Nonlinear Control*, 2024.

[11] P. Aschner et al. The international diabetes federation's guide for diabetes epidemiological studies. *Diabetes Research and Clinical Practice*, 172, 2021.

[12] M. A. Atkinson, G. S. Eisenbarth, and A. W. Michels. Type 1 diabetes. *The Lancet*, 383(9911):69–82, 2014.

[13] C. Cobelli, E. Renard, and B. Kovatchev. Artificial pancreas: Past, present, future. *Diabetes*, 60(11):2672–2682, 2011.

[14] P. E. Cryer et al. Hypoglycemia, functional brain failure, and brain death. *J. Clin. Invest.*, 117(4):868–870, 2007.

[15] J. C. Pickup, H. Keen, J. A. Parsons, and K. G. M. M. Alberti. Continuous subcutaneous insulin infusion: An approach to achieving normoglycaemia. *Br. Med. J.*, 1:204–207, 1978.

[16] F. J. Doyle, L. M. Huyett, J. B. Lee, H. C. Zisser, and E. Dassau. Closed-loop artificial pancreas systems: Engineering the algorithms. *Diabetes Care*, 37(5):1191–1197, 2014.

[17] C. K. Boughton and R. Hovorka. Advances in artificial pancreas systems. *Science Translational Medicine*, 11(484):eaaw4949, 2019.

[18] A. Cinar. Artificial pancreas systems: An introduction to the special issue. *IEEE Control Systems Magazine*, 38(1):26–29, 2018.

[19] M. E. Fisher. A semiclosed-loop algorithm for the control of blood glucose levels in diabetics. *IEEE Trans. Biomed. Eng.*, 38:57–61, 1991.

[20] C. Dalla Man, R. A. Rizza, and C. Cobelli. Meal simulation model of the glucose–insulin system. *IEEE Trans. Biomed. Eng.*, 54:1740–1749, 2007.

[21] A. Facchinetti, S. Del Favero, G. Sparacino, J. R. Castle, W. K. Ward, and C. Cobelli. Modeling the glucose sensor error. *IEEE Trans. Biomed. Eng.*, 61(3):620–629, 2013.

[22] G. M. Steil, K. Rebrin, C. Darwin, F. Hariri, and M. F. Saad. Feasibility of automating insulin delivery for the treatment of type 1 diabetes. *Diabetes*, 55:3344–3350, 2006.

[23] E. Ruiz Velázquez, R. Femat, and D. Campos-Delgado. Blood glucose control for type I diabetes mellitus: A robust tracking h_∞ problem. *Control Engineering Practice*, 12(9):1179–1195, 2004.

[24] B. W. Bequette. Algorithms for a closed-loop artificial pancreas: The case for model predictive control. *J. Diabetes Sci. Technol.*, 7(6):1632–1643, 2013.

[25] D. Boiroux et al. Adaptive control in an artificial pancreas for people with type 1 diabetes. *Control Engineering Practice*, 58:332–342, 2017.

[26] M. R. Askari et al. Adaptive-learning model predictive control for complex physiological systems: Automated insulin delivery in diabetes. *Annual Reviews in Control*, 50:1–12, 2020.

[27] S. A. Babar, I. Ahmad, and I. S. Mughal. Sliding-mode-based controllers for automation of blood glucose concentration for type 1 diabetes. *IET Systems Biology*, 15(2):72–82, 2021.

[28] M. Djouima, A. T. Azar, S. Drid, and D. Mehdi. Higher order sliding mode control for blood glucose regulation of type 1 diabetic patients. *Int. J. System Dynamics Applications*, 7(1):65–84, 2018.

[29] O. Hachana et al. Terminal synergetic controller for blood glucose regulation in diabetic type I patients. *ASME J. Dyn. Syst. Meas. Control*, 2018.

[30] S. A. Babar, I. A. Rana, I. S. Mughal, and S. A. Khan. Terminal synergetic and state feedback linearization based controllers for artificial pancreas in type 1 diabetic patients. *IEEE Access*, 9:28012–28019, 2021.

[31] S. A. Babar, I. A. Rana, M. Arslan, and M. W. Zafar. Integral backstepping based automated control of blood glucose in diabetes mellitus type 1 patients. *IEEE Access*, 7:173286–173293, 2019.

[32] I. Ahmad, F. Munir, and M. F. Munir. An adaptive backstepping based non-linear controller for artificial pancreas in type 1 diabetes patients. *Biomedical Signal Processing and Control*, 47:49–56, 2019.

[33] S. Sepasi, A. A. Kalat, and M. Seyedabadi. An adaptive back-stepping control for blood glucose regulation in type 1 diabetes. *Biomedical Signal Processing and Control*, 66:102498, 2021.

[34] R. Zahedifar and K. A. Keymasi. Control of blood glucose induced by meals for type-1 diabetics using an adaptive backstepping algorithm. *Scientific Reports*, 12(1):12228, 2022.

[35] S. Das, A. Nath, R. Dey, and S. Chaudhury. Glucose regulation in diabetes patients via insulin pump: A feedback linearisation approach. *Innovations in Infrastructure: Proceedings of ICIIF 2018*, pages 55–65, 2019.

[36] B. Farahmand, M. Dehghani, and N. Vafamand. Fuzzy model-based controller for blood glucose control in type 1 diabetes: An lmi approach. *Biomedical Signal Processing and Control*, 54:101627, 2019.

[37] J. L. C. B. de Farias and W. M. Bessa. Intelligent control with artificial neural networks for automated insulin delivery systems. *Bioengineering*, 9(11):664, 2022.

[38] L. Dénes-Fazakas et al. Control of type 1 diabetes mellitus using direct reinforcement learning based controller. In *2022 IEEE Intl. Conf. Systems, Man, Cybernetics*, pages 1512–1517, 2022.

[39] N. Vafamand, M. H. Asemani, S. Mobayen, and G. Pujol-Vázquez. Adaptive model reference control system integrated with modified smith predictor for glucose regulation. *IEEE Trans. Syst. Man Cybern.*, 2021.

[40] S. Faccioli et al. Super-twisting-based meal detector for type 1 diabetes management. *Computer Methods and Programs in Biomedicine*, 219:106736, 2022.

[41] J. Deichmann and H.-M. Kaltenbach. Model predictive control to account for prolonged changes in insulin requirements following exercise in type 1 diabetes. *J. Process Control*, 129:103042, 2023.

[42] A. Beneyto, A. Bertachi, J. Bondia, and J. Vehi. A new blood glucose control scheme for unannounced exercise in type 1 diabetic subjects. *IEEE Trans. Control Syst. Technol.*, 28(2):593–600, 2018.

[43] C. M. Ramkissoon, B. Aufderheide, B. W. Bequette, and J. Vehí. A review of safety and hazards associated with the artificial pancreas. *IEEE Reviews in Biomedical Engineering*, 10:44–62, 2017.

[44] Howard Kaufman, Itzhak Barkana, and Kenneth Sobel. *Direct Adaptive Control Algorithms: Theory and Applications*. Springer, New York, 2 edition, 1998.

[45] Kenneth M. Sobel, Howard Kaufman, and Lawrence Mabius. Implicit adaptive control for a class of MIMO systems. *IEEE Trans. Aerospace Electron. Syst.*, AES-18:675–690, 1982.

[46] Itzhak Bar-Kana. Almost passivity and simple adaptive control of nonstationary continuous linear systems. *Int. J. Syst. Sci.*, 21:835–862, 1990.

[47] B. W. Bequette. *Process Control: Modeling, Design and Simulation*. Prentice Hall, 2012.

[48] R. N. Bergman, Y. Z. Ider, C. R. Bowden, and C. Cobelli. Quantitative estimation of insulin sensitivity. *Am. J. Physiol.*, 236:E667–E677, 1979.

[49] P. A. Ioannou and P. V. Kokotovic. Instability analysis and improvement of robustness of adaptive control. *Automatica*, 20:583–594, 1984.